

Nation-wide mapping of tree level carbon stocks in Rwanda

Maurice Mugabowindekwe

Københavns Universitet

Martin Brandt (✉ martin.brandt@mailbox.org)

Københavns Universitet <https://orcid.org/0000-0001-9531-1239>

Jerome Chave

CNRS, Université Paul Sabatier <https://orcid.org/0000-0002-7766-1347>

Florian Reiner

Københavns Universitet

David Skole

Michigan State University <https://orcid.org/0000-0002-8575-3540>

Ankit Kariyaa

Københavns Universitet

Christian Igel

University of Copenhagen <https://orcid.org/0000-0003-2868-0856>

Pierre Hiernaux

Københavns Universitet

Philippe Ciais

Laboratoire des Sciences du Climat et de l'Environnement <https://orcid.org/0000-0001-8560-4943>

Ole Mertz

University of Copenhagen <https://orcid.org/0000-0002-3876-6779>

Xiaoye Tong

University of Copenhagen

Sizhuo Li

Københavns Universitet

Gaspard Rwanyiziri

University of Rwanda

Thaulin Dushimiyimana

Københavns Universitet

Alain Ndoli

International Union for Conservation of Nature

Valens Uwizeyimana

Department of Earth and Environmental Sciences <https://orcid.org/0000-0003-0120-9837>

Jens-Peter Lillesø

University of Copenhagen <https://orcid.org/0000-0003-1418-3496>

Fabian Gieseke

University of Münster

Compton Tucker

NASA

Sassan S Saatchi

University of California Los Angeles

Rasmus Fensholt

University of Copenhagen <https://orcid.org/0000-0003-3067-4527>

Article

Keywords:

Posted Date: June 1st, 2022

DOI: <https://doi.org/10.21203/rs.3.rs-1536453/v1>

License:  This work is licensed under a Creative Commons Attribution 4.0 International License.

[Read Full License](#)

Nation-wide mapping of tree level carbon stocks in Rwanda

Maurice Mugabowindekwe^{1,2}, Martin Brandt¹, Jérôme Chave³, Florian Reiner¹, David L. Skole⁴, Ankit Kariryaa^{1,5}, Christian Igel⁵, Pierre Hiernaux⁶, Phillippe Ciaï⁷, Ole Mertz¹, Xiaoye Tong¹, Sizhuo Li^{1,8}, Gaspard Rwanyiziri^{2,9}, Thaulin Dushimiyimana¹, Alain Ndoli¹⁰, Valens Uwizeyimana^{11,12}, Jens-Peter Barnekow Lillesø¹, Fabian Gieseke^{5,13}, Compton J. Tucker¹⁴, Sassan Saatchi¹⁵, Rasmus Fensholt¹

¹ Department of Geosciences and Natural Resource Management, University of Copenhagen, Copenhagen, Denmark

² Centre for Geographic Information Systems and Remote Sensing, College of Science and Technology, University of Rwanda, Kigali, Rwanda

³ Laboratoire Evolution et Diversité Biologique, CNRS, UPS, IRD, Université Paul Sabatier, Toulouse, France

⁴ Global Observatory for Ecosystem Services, Department of Forestry, Michigan State University, East Lansing, MI 48823, USA

⁵ Department of Computer Science, University of Copenhagen, Copenhagen, Denmark

⁶ Pastoralisme Conseil, Caylus, France

⁷ Laboratoire des Sciences du Climat et de l'Environnement, CEA/CNRS/UVSQ/Université Paris Saclay, Gif-sur-Yvette, France

⁸ Université Paris Saclay, Gif-sur-Yvette, France

⁹ Department of Geography and Urban Planning, College of Science and Technology, University of Rwanda, Kigali, Rwanda

¹⁰ International Union for Conservation of Nature, Kigali, Rwanda

¹¹ General Directorate of Land, Water, and Forestry, Ministry of Environment, Kigali, Rwanda

¹² Department of Earth and Environmental Sciences, Division of Forest, Nature and Landscape, KU Leuven. Celestijnenlaan 200E, B-3001, Leuven, Belgium

¹³ Department of Information Systems, University of Münster, Münster, Germany

¹⁴ Earth Sciences Division, NASA Goddard Space Flight Center, Greenbelt, MD 20771, USA

¹⁵ Jet Propulsion Laboratory, California Institute of Technology, Pasadena, CA 91109, USA

Abstract

Trees sustain livelihoods and mitigate climate change, but a predominance of trees outside forests and limited resources make it difficult for many developing countries to conduct frequent nation-wide inventories. Here, we propose a rapid and accurate approach to map the carbon stock of each individual tree and shrub at the national scale of Rwanda using aerial imagery and deep learning. We show that 72% of the mapped trees are located in farmlands and savannas, and 15% in plantations. These non-forest trees account for 41% of the national carbon stocks. Natural forests cover 5% of the country and 11% of the total tree count, but comprise 59% of the national carbon stocks. The mapping of all trees facilitates any landscape stratification and is urgently needed for effective planning and monitoring of landscape restoration activities as well as for optimization of carbon sequestration, biodiversity and economic benefits of trees.

Introduction

Trees both inside and outside forests are the foundation of ecosystem structure and function (1). Individual tree traits such as size and spatial distribution are key determinants of ecosystem services such as carbon storage, climate regulation, food security, and fuel wood (2,3). Because of their strategic importance, countries across the globe regularly evaluate, quantify and monitor forests using field inventories as part of national forest monitoring systems (4-6). Forest inventories are the backbone to measurement, reporting and validation (MRV) for international climate change mitigation initiatives such as national level REDD+ (Reducing Emissions from Deforestation and Forest Degradation) (5,6), Sustainable Development Goals (SDGs) especially SDG no. 15 (7), the Paris Agreement (8), and the Bonn Challenge (9). In European countries, sample-based forest inventories are often accompanied by airborne

46 LiDAR campaigns, providing detailed information on the carbon stocks of forests. However, field inventories and
47 LiDAR campaigns are expensive and labour-intensive (4), resulting in trade-offs between accuracy, reproducibility,
48 and the frequency of reporting. In developing countries, financial and human resource constraints limit the coverage
49 and frequency of the field inventories.

50 This is particularly problematic for many African countries, where LiDAR data are not available across a variety of
51 landscape types, ranging from savannas, woodlands, sub-humid and humid forests, to highly fragmented, small scale
52 agro-ecosystem mosaics. This complexity makes it difficult to scale from sparsely sampled plots to the national
53 scale. Indeed, many of these landscapes are dominated by non-forest trees which are very difficult to map with
54 traditional methods (10,11).

55 Inventories and existing large-scale tree cover maps (12-14) often omit an accurate accounting of trees growing
56 outside forests, which is related to differences in forest definitions, mapping techniques, and the complexity of the
57 environment (15,16). This leads to incomplete censuses of trees and their related benefits and services at a national
58 scale (16). More specifically, these inaccuracies aggravate the existing uncertainties in estimates of both national
59 carbon stocks and emission reference levels (17,18), and may confound the relative contributions of emissions
60 attributed to forest degradation or deforestation (19). In turn, these inaccuracies in tree mapping hinder natural
61 resource management and climate change decision-making and policy-formulation (20). These challenges are
62 especially significant in the tropics, where a large number of important landscape restoration activities and projects
63 have been initiated without fully functional monitoring systems in place (21,22).

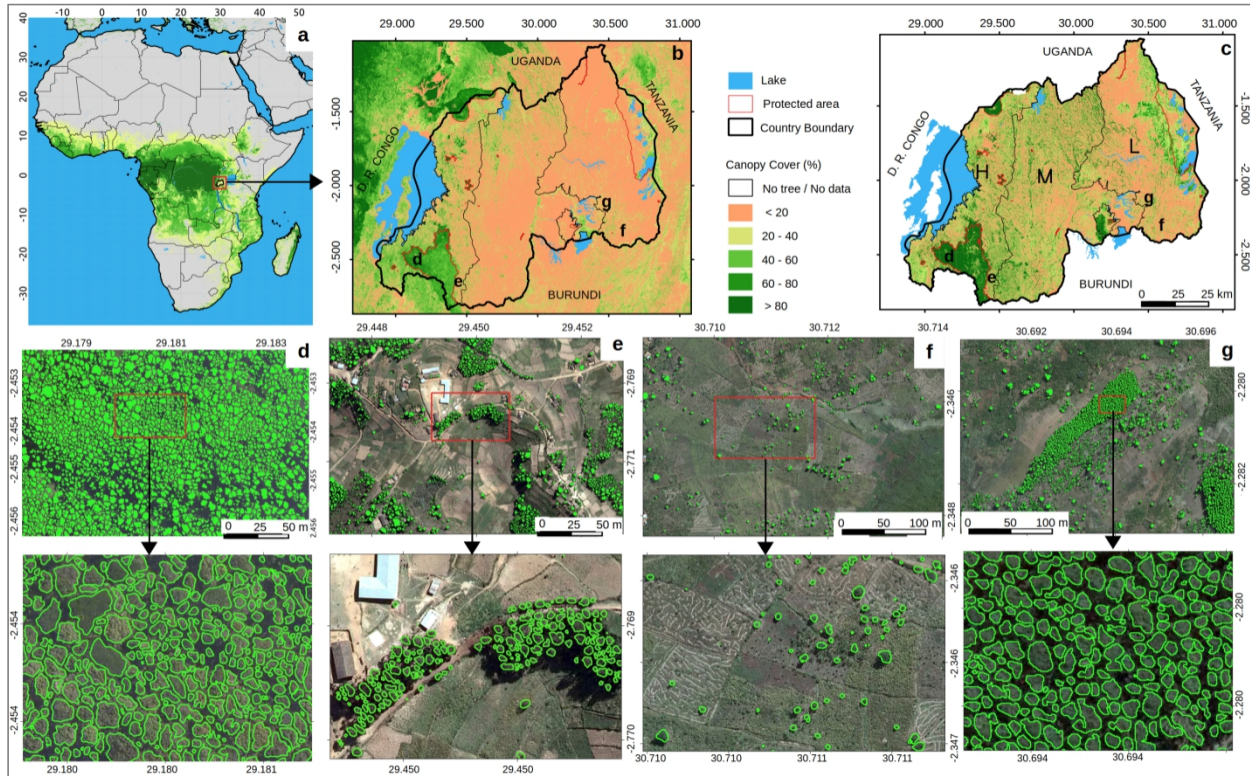
64 In Africa, the alarming rate of tree cover loss has spurred both political and economic incentives for the restoration
65 of tree-dominated landscapes (14,23,24). Ongoing initiatives include the African Forest Landscape Restoration
66 Initiative (AFR100), with more than 30 African governments making commitments to restore at least 100 million
67 hectares of land across the continent by 2030 (21), the African Resilient Landscapes Initiative (ARLI), the Africa
68 Low Emissions Development Strategies (25), among others. However, there is currently no accurate and regularly
69 updated monitoring platform to track the progress and biophysical impact of these initiatives (26). Here, we propose
70 an approach to rapidly and accurately map individual trees and quantify their carbon stocks at national scale, and
71 illustrate how some of the above-mentioned challenges can be addressed with efficient new monitoring tools, using
72 Rwanda as a case study. The country has been selected based on two key criteria. First, it is a signatory to most of
73 the above-mentioned global climate mitigation initiatives and regularly reports on their implementation. Rwanda
74 had targeted at least 30% of the country to be covered by forests by the year 2020 (27,28), which was achieved in
75 2019 (29). Under the Bonn Challenge, the country has also committed to restore 2 million hectares by 2030, or 81%
76 of the country's surface area (30). Second, although the country is small in size, it represents contrasting landscape
77 types and land uses: drylands dominated by savannas and pastureland, plateaus dominated by agriculture, and humid
78 highlands dominated by natural forests and protected areas, including tropical montane rainforest (31, 32).

79 Recently, (15) demonstrated that advanced machine learning techniques are able to map individual trees over large
80 dryland areas. However, the analysis used costly commercial satellite images, was limited to isolated trees in
81 savannas excluding small trees with a crown area below 3 m², and did not cover other complex and heterogeneous
82 ecosystems such as woodlands and forests. Here, we use publicly available aerial images and map the crown size
83 and carbon stock of each individual tree in Rwanda, regardless of ecosystem type. We suggest a rapid, reproducible
84 and highly accurate way to upscale field inventory data collected at the level of individual trees to the entire country.
85 This will allow tree inventory reports to be of unprecedented accuracy, and can support MRV of climate change
86 mitigation initiatives. The repeated reporting at the level of individual trees also enables the distinction between tree
87 harvest, deforestation and forest degradation, which can then be linked to land use and ownership, payment of
88 ecosystem services, logging permit issuance and compliance, among other benefits.

89 **Results**

90 **Comprehensive mapping of individual trees at national scale.** Aerial images with a spatial resolution of 25x25
91 cm were acquired in 2008 covering the entire country (33). A deep learning model was trained using 97,574 hand-

92 labeled tree crowns and then used to map 357,437,805 trees with a crown size larger than 0.25 m². The crown area
 93 threshold was set based on visual inspection of the images, as trees of this size are still clearly visible (Fig. 1). To
 94 separate clumped crowns, we developed a post-processing method to determine the crown centers in the predictions,
 95 assuming that tree crowns have round shapes. The method then relabels the crown predictions based on weighted
 96 distances to the identified crown centers (see Methods).

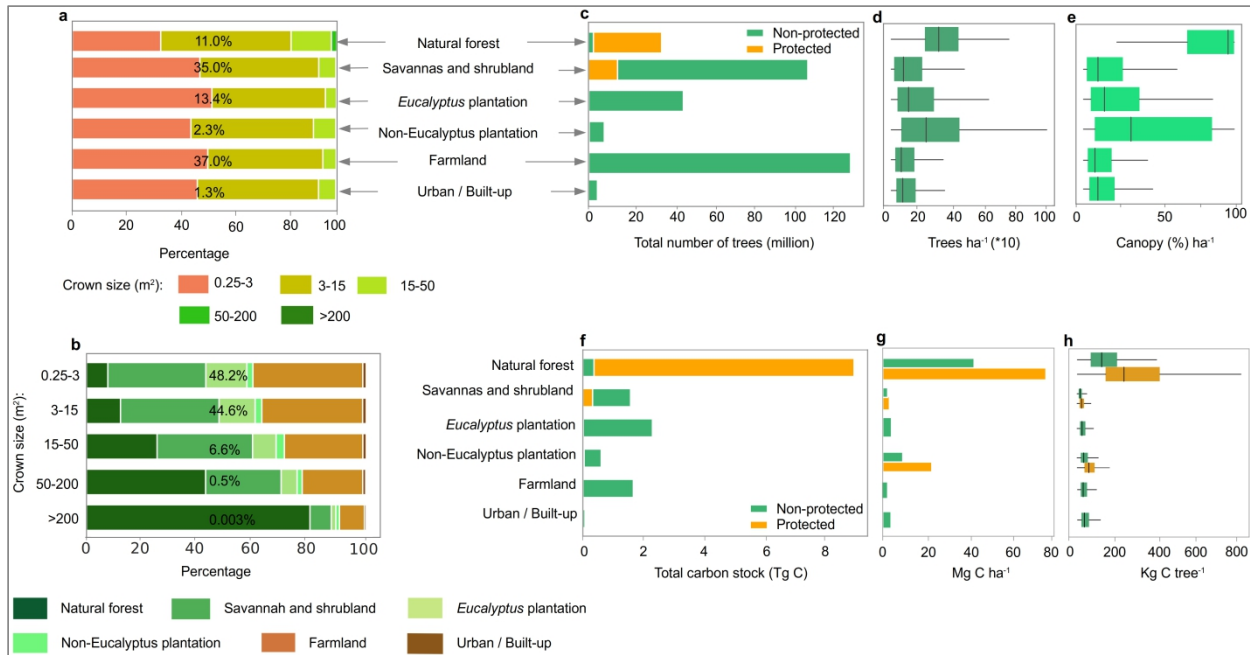


97

98 **Fig. 1. Mapping of individual trees inside and outside of forests in Rwanda.** a, Tree cover from a previously
 99 published global tree cover map using Landsat data (12) in Africa and b, in Rwanda. c, Country-wide tree cover
 100 estimated by deep learning from 0.25 m resolution aerial imagery from 2008 (L: Lowlands, M: Midlands, H:
 101 Highlands). d-e, Examples of individual tree crown mapping in d, tropical montane rainforest; e, *Eucalyptus*
 102 plantations; f, farmlands; and g, *Pinus* plantations. An example of previously published manual forest area
 103 delineations is shown in Extended Data | Fig. 1.

104 Following a manual delineation, which is also based on the same aerial images as used here and includes forest
 105 patches down to a size of 0.25 ha (34; Extended Data | Fig. 1), we stratified the landscapes into natural forest,
 106 *Eucalyptus* plantations (excluding isolated *Eucalyptus* trees in farmlands and urban areas), non-*Eucalyptus* tree
 107 plantations, farmlands, urban areas (including all the built-up areas), as well as savannas and shrublands (see
 108 Methods). We further subdivided each class in protected and non-protected areas (31). Overall, our results show a
 109 dominance of trees with small crown sizes of 0.25-3 m² which account for 48.2% of the mapped trees, followed by
 110 crown sizes of 3-15 m² which account for 44.6% of the trees. Related to our land stratification, these two crown size
 111 ranges are dominant in farmlands and *Eucalyptus* plantations (Fig. 2a,b). Trees of the largest crown size class
 112 (crown sizes > 200 m²) are very scarce and mainly found in natural forests which dominate areas under protection.

113



114

115 **Fig. 2. Tree counts, crown areas and carbon stocks for different land cover/use types.** a, Percentage covered by
 116 different crown sizes in each land cover/use type. The percent number shows the contribution of the land cover/use
 117 type to the total area. Crown sizes >200 m² comprise only 0.003% of the total tree count, making the class barely
 118 visible. b, Percentage covered by each land cover/use type in different crown size categories. c, Total count of trees
 119 by land cover/use. d, Boxplot showing the average number of trees per ha by land cover/use type. e, As d but for
 120 canopy cover. f, Total estimated carbon stock per land cover/use type (see Methods for uncertainties and error
 121 propagation), g, barplot showing the average carbon density per ha per land cover/use. h, Boxplots showing the
 122 average carbon stock per tree per land cover/use. Number of trees = 357,437,805.

123 **Table 1. Tree counts in the major landscape types of Rwanda**

Landscape type	Biophysical and climatic characteristics	Area and tree count (total & %)	Trees ha ⁻¹ - median (5 th - 95 th)	Canopy cover (%) ha ⁻¹ - median (5 th - 95 th)
Lowlands	- Elevation range: 900-1,500 m - Mean annual rainfall: 600 - 2000 mm - Mean annual temperature: 17 - 24°C - Dominant tree-dominated cover type: savanna and tree plantations	- Area: 984,575 ha (38.9%) - Tree count: 95,071,194 (26.6%)	53(0-350)	6.2(0-54.4)
Midlands	- Elevation range: 1500-2000 m - Mean annual rainfall: 1300-2200 - Mean annual temperature: 14 - 24°C - Dominant tree-dominated cover type: tree plantations	- Area: 1,084,908 ha (42.8%) - Tree count: 157,941,607 (44.2%)	86(8-478)	10.9(0.7-80.7)
Highlands	- Elevation range: 2000-4,507 m - Mean annual rainfall: 1800-2300 mm - Mean annual temperature: 8 - 21°C - Dominant tree-dominated cover type: tropical montane rainforest and forest plantations	- Area: 463,382 ha (18.3%) - Tree count: 104,425,004 (29.2%)	165(7-632)	20.4(0.3-100)

124 **Tree counts and densities for different landscape types and land uses.** Elevation and rainfall are key
125 determinants of ecosystem structure in Rwanda (31,32) and are closely related with the distribution of trees (Table 1;
126 Extended Data | Fig. 2). The highlands cover the smallest area of the country (18.3%) but have the highest tree
127 density and canopy cover. They are also home to the largest tropical montane rainforest of the country, located
128 inside a protected area, the Nyungwe National Park in the South-West. Protected forests in highlands account for
129 9.5% of the total mapped trees and 42.5% of the national carbon stock.

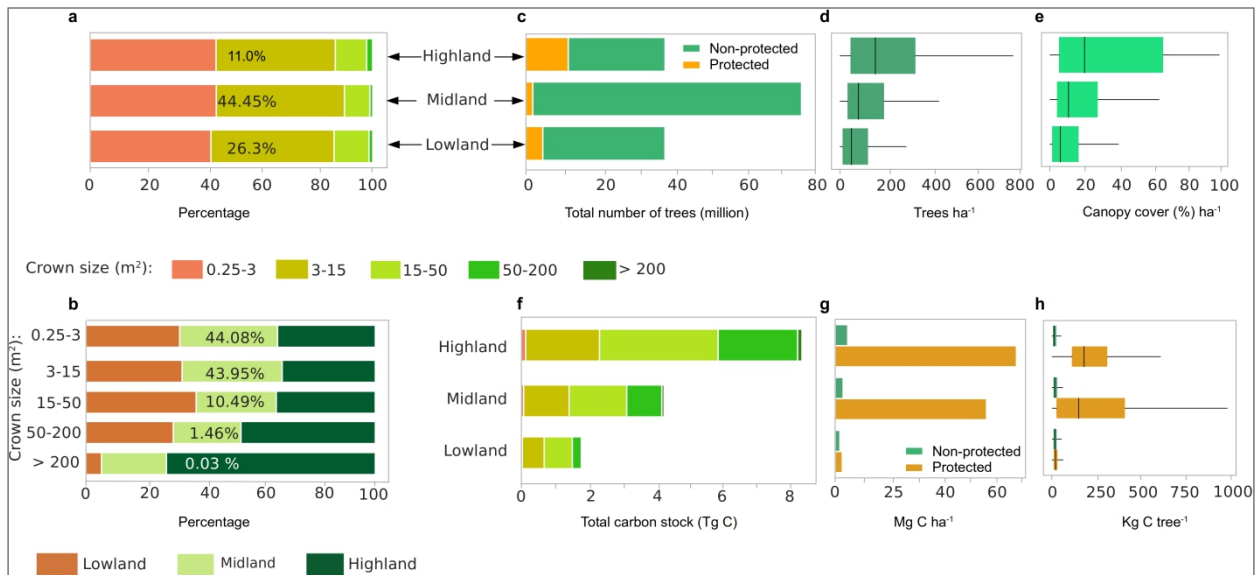
130 We show that 11% of the mapped trees are located inside natural forests, and the largest number of trees are located
131 in farmland (37%). Specifically, natural forests have 39.3 million trees, with a median (5th-95th percentiles) density
132 of 298 (42-580) trees ha⁻¹, and a median canopy cover of 96% (1.8-100%). Farmlands have a median tree density of
133 63 (4-411) trees ha⁻¹ and a median canopy cover of 7.6% (0-57.4%). *Eucalyptus* plantations account for about 48
134 million trees (~13.4% of the total mapped trees), a median density of 109 (9-598) trees ha⁻¹, and median canopy
135 cover of 13.9% (0.7-85.1%). The low canopy cover can be explained by the inclusion of bare areas manually
136 delineated as plantation areas (Extended Data | Fig. 1). Non-*Eucalyptus* tree plantations have 8.3 million trees
137 (~2.3% of the total mapped trees), a median density of 219 (11-670) trees ha⁻¹ and a median canopy cover of 31.5%
138 (0.9-100%). Urban areas have 4.5 million trees (~1.3% of the total mapped trees), and a median density of 72 (5-429)
139 trees ha⁻¹. Savannas and shrublands account for 125.1 million trees (~35% of the total mapped trees), with a median
140 density of 77 (0-478) trees ha⁻¹ and a median canopy cover of 9.6% (0-72.7%). Overall, trees outside of natural
141 forests cover 318.1 million trees, of which 41.6% are in farmlands. The quantification of non-forest trees depends on
142 how forests are defined. If we would consider both natural forests and tree plantations as forest, 73.3% of the trees in
143 Rwanda would be considered as trees outside forests. Using our own tree cover map and consider areas with canopy
144 cover above 25% (10%) as forest, 53.9% (31.8%) would be trees outside forests.

145 The importance of protected areas for tree density and count is worthwhile to note. Although they cover only 9% of
146 the country, they have 52.1 million trees (11% of the total mapped trees) with the highest median tree density of 206
147 (0-553) trees ha⁻¹ and median canopy cover of 44.1% (0-100%). Overall, we show that 20.8% of Rwanda was
148 covered by trees (canopy cover) in 2008. Note that understory trees are not visible in aerial/satellite images (see
149 Methods).

150 **Carbon stocks estimated for individual trees.** We conducted a field campaign in December 2021 and measured
151 793 trees in the natural forest, and also used 10,591 measurements of non-forest trees from (35), as well as 952 non-
152 forest trees from (36) to estimate the stem diameter from the mapped crown sizes via allometric equations. We then
153 estimated the above-ground carbon stocks for each tree using existing equations (see Methods). We established
154 biome specific relationships and report here the combined results from (37) for natural forest; (38) for *Eucalyptus*
155 and non-*Eucalyptus* plantations, farmlands, and urban areas; and (36) for savannas and shrublands. For each biome,
156 we validated the results with data from the Rwanda National Forest Inventory (NFI) from 2013/2014 as well as with
157 field measurements from Kenya and Rwanda (see Methods). From these field data, we estimate an overall area
158 weighted C stock uncertainty of 16.9% at national scale: 5.9% for farmlands, 18.9% for savannas and shrublands,
159 26% for natural forests, and 52.6% for plantations (see Methods for sources of uncertainties). The high uncertainty
160 for plantations can be partly explained by the time difference between images and field data and the inaccuracies in
161 the manual delineation of plantation areas (Extended Data | Fig. 1). We estimate a total of 34.9 Tg of dry matter
162 content from stems, branches and leaves of the mapped trees across the country, which represents an equivalent of
163 16.4 Tg of above-ground carbon stocks. For areas outside the natural forests, we estimate 7.0 Tg C, which is 42.3%
164 of the total national carbon stocks and slightly lower than NFI estimations (8.4 Tg C). Farmlands have a total
165 estimate of 3.5 Tg C corresponding to 21.3% of the national C stock with a C density of 3.0 (0.1-9.1) Mg C ha⁻¹.
166 Urban areas have 0.1 Tg C corresponding to 0.9% of the national C stock with a C density of 4.0 (0.2-11.8) Mg C
167 ha⁻¹. *Eucalyptus* plantations comprise a total estimate of 1.1 Tg C corresponding to 6.8% of the national C stocks,
168 with a C density of 4.2 (0.2-12.6) Mg C ha⁻¹. These low estimates can be explained by the fact that regular
169 harvesting keeps the trees young (39) in addition to sparse tree planting practices in some cases (40). Non-
170 *Eucalyptus* plantations have a total estimate of 0.3 Tg C corresponding to 1.9% of the national carbon stocks, with a
171 C density of 10.0 (0.3-29.3) Mg C ha⁻¹. Savannas and shrublands have 1.9 Tg C corresponding to 11.7% of the
172 national C stock with a C density of 2.4 (0.0-7.4) Mg C ha⁻¹. For natural forests, we estimate a mean C density of

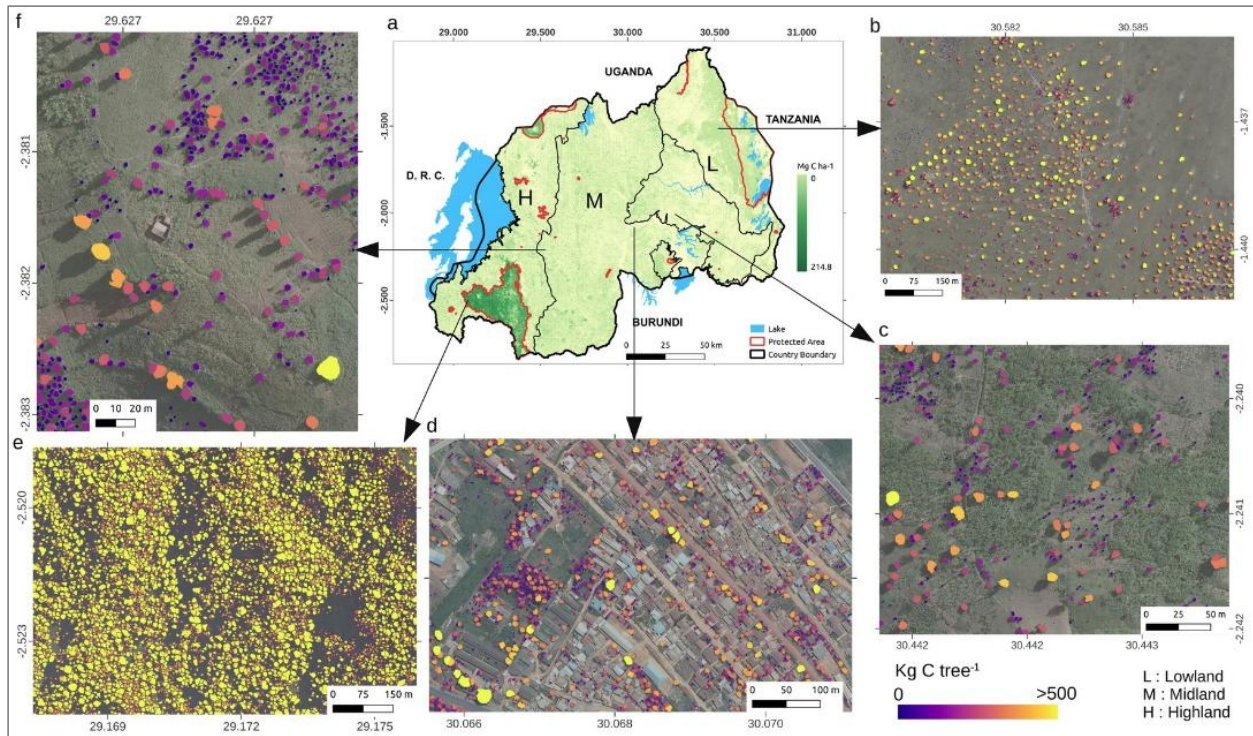
173 102.8 Mg C ha⁻¹ for areas where field data are available (i.e. Nyungwe tropical montane rainforest in South-west of
 174 Rwanda), which is lower than the field measurements of 139 Mg C ha⁻¹ (41,42), possibly due to trees from lower
 175 layers not being visible from above. Overall, we estimate that 58.7% of the total national carbon stocks are in natural
 176 forests with a total estimate of 9.5 Tg C and a C density of 75.9 (3.6-142.1) Mg C ha⁻¹.

177 The highlands have an overall estimate of 8.7 Tg C with mean C density of 18.8 (0.1-102.8) Mg C ha⁻¹. The
 178 midlands have a total estimate of 5.3 Tg C with mean C density of 4.9 (0.2-10.8) Mg C ha⁻¹, while the lowlands
 179 contain a total estimate of about 2.4 Tg C with mean C density of 2.8 (0.0-8.6) Mg C ha⁻¹. Overall, our results show
 180 that carbon stocks highly increase with both increase in density and cover of large trees, compared to an increase in
 181 small trees (Extended Data | Fig. 2). Using our own tree cover map and considering areas with a canopy cover above
 182 25% (10%) as forest, 28.9% (16.9%) of the national C stocks would be stored in trees outside forest.



183
 184 **Fig. 3. Tree properties of different landscape types.** **a**, Percentage covered by different crown sizes in each
 185 landscape type. The percent number shows the contribution of the landscape type to the total area. **b**, Percentage
 186 covered by each landscape type in different crown size categories. **c**, Total count of trees by landscape type. **d**,
 187 Boxplot showing the average number of trees per ha by landscape type. **e**, Same as **d** but for tree cover. **f**, Total
 188 estimated carbon stock per landscape type. **g**, Barplots showing the distribution of average carbon stock per ha per
 189 landscape type, and **h**, boxplots showing the average the carbon stock per tree per landscape type.

190



191

192 **Fig. 4. Above-ground carbon stocks at tree level in Rwanda. a**, Spatial distribution of the estimated carbon stock
 193 across the major landscape types. **b-f**, Examples of estimated carbon stock per individual tree in, **b**, wooded savanna,
 194 **c**, farmland, **d**, Kigali city, **e**, the tropical montane rainforest in the Nyungwe National Park, and **f**, in tree
 195 plantations.

196 **Discussion**

197 We report on a country-scale comprehensive mapping of individual trees both inside and outside forests for Rwanda,
 198 a country that spans a wide range of African landscapes: natural forest - including tropical montane rainforest,
 199 savannas and shrublands, tree plantations (including young plantations and coppices), agroforestry trees in
 200 farmlands, and isolated garden trees. Using aerial images and deep learning, we have demonstrated that we are
 201 able to quantify the spatial distribution and carbon stock of all trees and shrubs of the country, down to crown sizes as
 202 small as 0.25 m².

203 Assessments and reporting schemes of tree resources at country scale are limited by poor data quality and
 204 ambiguous or inconsistent definitions of land cover and land use types (20,43). Forests have been defined differently
 205 depending on location, measurement protocols, and landscape contexts. When forests are specified as continuous
 206 tree cover at a given mapping resolution, the underlying definition and the quality of the data product are essential to
 207 understand precisely what is being mapped. For instance, at medium spatial resolution, tree cover products may
 208 include only continuous clusters of trees of a certain size, and may exclude shrubs and isolated trees. Ambiguities
 209 and uncertainties also result from differences in the quality of the data (12). A previous work has overestimated the
 210 extent of forests by the inclusion of shrubs and bushes as forestland (44). Uncertainties in tree cover estimates
 211 propagate to estimations of carbon stocks, resulting in large uncertainties in existing biomass and carbon estimates
 212 and maps (45, Extended Data | Fig. 4).

213 This analysis presents an assessment of all trees, aside the assessment of their cover, density or land use, allowing
 214 for an accurate and independent quantification of the woody resources and carbon stocks. Thus, another major
 215 advance of the present study is that our carbon stocks are not merely proxy-based estimates per unit area, as it was
 216 the case of previous work. Rather, we map individual tree allometric parameters, especially tree crown area, and

217 calculate tree carbon stocks for each tree, an approach that previously was only possible with spatially limited field
218 inventory or LiDAR data (35). Most of allometric scaling from a tree parameter to biomass or carbon involves non-
219 linear relationships, where the size class distribution of trees matters for the final estimate of landscape carbon
220 stocks. This large national-scale analysis provides the distribution of tree sizes and thereby is directly useful for
221 application with standard or local allometric models.

222 Furthermore, the ability to map all trees makes our assessment independent of forest, tree cover and land use
223 definitions. Reporting carbon stocks based on individual trees would solve important uncertainties caused by
224 definitions, methods, data sources, and spatial resolution (20). Our example shows that even a very detailed manual
225 forest delineation approach missed 38.2% of the isolated trees in Rwanda, which account for 22.2% of the national
226 carbon stocks and likely a larger fraction of growing stocks. With results as presented here, management and
227 conservation decision-making can be more targeted by discriminating various types of tree systems under specific
228 conditions and in specific locations. Our approach therefore could support management of a broad array of tree-
229 based systems such as agroforestry and farmer managed regeneration, as well as catalyze important cross-sector
230 management strategies inclusive of Agriculture, Forestry and other Land Use (AFoLU). A focus on AFoLU
231 provides a way to simultaneously manage both emission reductions and removals of greenhouse gases (46).
232 Integrating non-forest trees along with trees inside forests in environmental conservation initiatives could be an
233 opportunity to expand the scope of ongoing climate change mitigation and adaptation efforts, such as various
234 approaches to REDD+ and the Bonn challenge for forest restoration by also accounting for trees not included in
235 standard forest assessments (47). Our methods would also provide much more effective, accurate, and regular
236 monitoring, though this will not solve the inherent problems in REDD+ of measuring emission reductions against
237 forest reference levels and counter-factual business as usual scenarios (17).

238 We can draw on a common concrete example of the value of discriminating tree-system types by looking at activity
239 data on forest area change. If only forest area or tree cover are reported, a cleared forest that is replaced by newly
240 planted trees might readily be treated as no net change, ignoring the loss in carbon in these areas during their
241 clearing. Interestingly, 54.2% of the mapped trees in Rwanda are plantations. Most of these trees were part of
242 Rwanda's phased out vision 2020 (28) and currently part of the Bonn Challenge, but their frequent harvest and
243 replanting keep their carbon stocks very low (3.4 Mg C ha⁻¹; 5.1 Tg C). This is contrasted by high numbers of
244 natural forests (11% of national tree count) which make up only 4.9% of Rwanda but store 58.7% of the national
245 carbon stocks (75.9 Mg C ha⁻¹; 9.5 Tg C, Extended Data | Fig. 8). While previous governmental programs aimed at
246 maximizing tree cover, results like shown in this study with the ability to attribute individual trees to their respective
247 land cover and use, can help to revise ongoing initiatives towards maximizing the sequestration of carbon.

248 Obtaining accurate individual tree maps depends on the availability of high-resolution satellite or aerial images.
249 While these data exist for many African countries, they are often old, and have not been digitized. Sometimes also
250 data access is restricted even for research (48), because images were acquired in the frame of sensitive information
251 such as land tenure or construction planning, and the data access rights remain with custodian institutions. Here we
252 show the benefits of such data for environmental applications, and how allocation of financial resources to their
253 acquisition can efficiently serve landscape monitoring and restoration efforts by providing more and better
254 information to support the monitoring, reporting and verification (MRV) efforts. In addition to directly supporting
255 national climate change mitigation efforts, accurate tree maps promote better understanding of the spatial
256 distribution and abundance of trees in relation to biophysical and climatic factors such as rainfall, temperature and
257 elevation (Extended Data | Fig. 2). The value of this is that climate change mitigation and adaptation actions can be
258 readily integrated into existing broad-based forest and sustainable land management plans and objectives.

259 We acknowledge that a satellite-based approach cannot resolve the full range of crown sizes in forests due to
260 overlapping crowns, and also the conversion of crown area to carbon stocks includes uncertainty (35,37,45) (see
261 Methods). However, our results are key to a better understanding of the structure and functioning of wooded
262 ecosystems, and vital for the development of informed regulation and monitoring policies for site- and ecosystem-
263 based interventions. To reduce uncertainty, future versions of the proposed method should include more localized
264 field inventory databases that allow for more local biome-specific allometric conversions, as well as integrate tree

265 height estimations from field and airborne LiDAR surveys. Ideally, national inventories are coupled with results
266 such as those presented here to identify systematic bias and optimize the upscaling from field plot information to
267 country scale.

268 Analyses as presented here quantify existing tree resources, and provide an example of an approach that empowers
269 countries to quantify carbon stocks at the level of individual trees (Fig. 4). Having this capability is important to a
270 range of applications including monitoring of forest landscape restoration, tree plantation survival rate, forest
271 demography: dynamics of mortality and recruitment, tree-dominated land ownership, payments for ecosystem
272 services, issuance of concession permits and tracking compliance, among other benefits. Therefore, we emphasize
273 the inclusion of funding for regular high resolution aerial/satellite imagery along with localized field inventory
274 databases in development packages. We also highlight the relevance of all trees for conservation and protection
275 efforts, and encourage that trees outside forests are considered as equally important as trees in forests.

276 **Methods**

277 **Aerial images.** We use publicly available aerial images of Rwanda at 0.25x0.25 m resolution, collected in June -
278 August of 2008 and 2009. The images were acquired from 3000 meter altitude above ground level, initially with a
279 mean ground resolution of 0.22x0.22 m pixel size, using a Vexcel UltraCam-X aerial digital photography camera
280 (33). They include a red, green, and blue band stored under 8 bit unsigned integer format. The aerial images cover
281 96% of the country, and the remaining 4% were filled by satellite images from WorldView-2, Ikonos, Spot, and
282 QuickBird satellite sensors which are part of the publicly available dataset.

283 **Environmental data.** We use locally available climate data: mean annual rainfall, mean annual temperature, and
284 elevation data (10x10 m resolution) to assess relationships between tree density, crown cover and environmental
285 gradients. We also use land cover data to extract the spatial extent of plantations, forest, farmland, and urban areas,
286 for our stratification. Climate data was obtained from the Rwanda Meteorological Agency as daily records from
287 1971 to 2017. The national forest map was manually created in 2012 using on-screen digitising techniques over the
288 2008 aerial images (34). A forest was defined as “a group of trees higher than 7 m and a tree cover of more than
289 10%, or trees able to reach these thresholds in situ on a land of about 0.25 ha or more” (49). A shrub was defined as
290 “a group of perennial trees smaller than 7 m at maturity and a canopy cover of more than 10% on a land of about
291 0.25 ha or more”. The forest dataset was composed of 105,690 forest polygons, classified as either natural forest (i.e.
292 closed natural forest, degraded natural forest, bamboo stand, wooded savanna, and shrubland), or “forest plantations”
293 (i.e. *Eucalyptus spp.* - Eucalyptus, *Pinus spp.* - pine, *Callitris spp.* - callitris, *Cupressus spp.* - cypress, *Acacia*
294 *mearnsii spp.* - black wattle, *Acacia melanoxylon* - melanoxylon, *Grevillea robusta* - grevillea, *Maesopsis eminii* -
295 maesopsis, *Alnus acuminata* - alnus, *Jacaranda mimosifolia* - jacaranda, mixed species - mixed, and others
296 (Extended Data | Fig. 9). We separate shrubland from natural forest and merged it with savanna into the class
297 “savannas and shrublands”. We further separated tree plantations and grouped them into *Eucalyptus* and non-
298 *Eucalyptus* plantations. Then, a farmland map was acquired from the Rwanda Land Management and Use Authority
299 (RLMUA) (50), and overlaid with the 2012 forest cover map as a reference to clean the overlapping parts, under an
300 assumption that the overlap is due to land use dynamics. Finally, a layer marking urban areas was acquired from
301 RLMUA as well, and the same pre-processing step as done for farmlands was applied. The combination of the land
302 cover datasets resulted in our stratification scheme with 6 classes: natural forests, savannas and shrublands,
303 *Eucalyptus* plantations, non-*Eucalyptus* plantations, farmland, and urban / built-up.

304 **Mapping of individual trees using deep learning.** We used the open-source framework developed by *ref. 15* to
305 map individual tree crowns. The framework uses a deep neural network based on the UNet architecture (51,52). We
306 trained the network using 97,574 manually delineated tree crowns spread over 103 areas/bounding boxes
307 representing the full range of biogeographical conditions found across Rwanda. To cope with the challenge of
308 separating touching tree crowns, we used a higher weight for boundary areas between crowns, as suggested in *ref 15*
309 and *ref. 51*. Crown sizes in the predictions were found to be 27% smaller as compared to the manual delineations
310 within the 103 training areas, which is caused by the applied boundary weight that emphasizes gaps between tree
311 crowns. Therefore, to calculate the real canopy cover, we extended each predicted tree crown by 27% and dissolved

312 the touching crowns into continuous features. Furthermore, we developed a post-processing method that separates
313 clumped tree crowns and fills any gap inside a single crown (Extended data | Fig. 7). Our post-processing method
314 determines the crown centers in the model predictions assuming that tree crowns have a round shape. The method
315 then relabels the model predictions based on weighted distances to the identified crown centers. We counted single
316 tree crowns for each hectare presented here as tree density, and the percentage of each hectare covered by the
317 extended tree crowns as canopy cover.

318 **Allometry for biomass and carbon stock estimation.** Generally, allometric equations define a statistical
319 relationship between structural properties of a tree and its biomass (53, 54). In our case, we assume a relationship
320 between the crown area and AGB, which varies between biomes (35). Since destructive AGB measurements are rare,
321 we established biome specific relationships between crown diameter (CD) derived from the crown area ($CD =$
322 $2 \cdot \sqrt{(\text{Crown area} / \pi)}$) and stem diameter at breast height (DBH) (E1,E4). DBH has been shown to be highly
323 correlated with AGB (36,37,45,53,54). We then used established relationships from literature to derive AGB from
324 DBH for savannas and shrublands (E2), tree plantations (E3), and natural forests (E5). AGB was predicted for each
325 tree and summed for 1 ha grids to derive AGB in the unit Mg per ha. Values were multiplied by 0.47 (55,56) to
326 derive above-ground carbon (AGC). Summed numbers over land cover classes are considered as carbon stocks. The
327 bias as reported here was calculated following the approach from *ref. 35* reporting relative absolute values.

328 For trees outside natural forests, we used the database from *ref. 35* including 10,591 field-measured trees from
329 woodlands and savanna plus 952 samples from agroforestry landscapes in Kenya (36) to establish a linear
330 relationship between CD and DBH (Extended Data | Fig. 3a). A major axis regression (average of 4 runs each 50%
331 of the data) leads to equation E1:

$$332 \text{DBH}_{\text{predicted}} \text{ in cm} = -4.665 + 5.102 * \text{CD} \text{ (E1)}$$

333 E1 shows a reasonable performance with a very low bias (average of 4 runs on the 50% not used to establish E1: $r^2 =$
334 0.71 ; slope = 0.95; RMSE = 6.2 cm = 42%; bias = 1%). We tested E1 on an independent data set from Kenya
335 consisting of 93 trees where AGB was destructively measured (Fig. 3b). On these 93 trees, DBH can be predicted
336 reasonably well from CD using E1 ($r^2 = 0.84$; slope = 0.86; RMSE = 8 cm = 25%; bias = 6%). We then applied an
337 allometric equation from literature (36) established for non forest trees in East Africa to estimate AGB from
338 $\text{DBH}_{\text{predicted}}$ and compared the predicted AGB with the destructively measured AGB ($r^2 = 0.81$; RMSE = 511 kg =
339 55%; bias = 25%) showing an acceptable performance (Extended Data | Fig. 3c) but indicating a systematic bias,
340 which will be further tested with biome specific field data (next section). We apply equation (E2) to estimate AGB
341 for trees outside forests in Rwanda in savannas and shrublands:

$$342 \text{AGB}_{\text{predicted}} \text{ in kg} = 0.091 * \text{DBH}_{\text{predicted}}^{2.472} \text{ (E2)}$$

343 Given the different structure of trees in farmlands, urban areas and plantations as compared to trees in natural forests
344 and in natural non-forest areas, we used a different equation for trees in these areas. It was established in Rwanda
345 using destructive samples from tree plantations (38):

$$346 \text{AGB}_{\text{predicted}} \text{ in kg} = 0.202 * \text{DBH}_{\text{predicted}}^{2.447} \text{ (E3)}$$

347 A different CD-DBH relationship was established for natural forests. Here we conducted a field campaign in
348 December 2021 sampling 793 overstorey trees in Rwanda's protected natural forest. We measured both CD and DBH
349 and established a logarithmic major axis regression with a Baskerville correction (57) between the two
350 variables to predict DBH from CD (Extended Data | Fig. 3d). We did 4 runs each using 50% of the data to establish
351 E4 (average of the 4 runs) and the other 50% to test the performance also averaged over the 4 runs ($r^2 = 0.71$; slope
352 = 0.99; RMSE = 13 cm = 45%; bias = 19%). Note that CD is extended by 27% to account for underestimations of
353 touching crowns in dense forests (see previous section):

$$354 \text{DBH}_{\text{predicted}} \text{ in cm} = (\exp(1.154 + 1.248 * \ln(\text{CD} * 1.27))) * (\exp(0.3315^{2/2})) \text{ (E4)}$$

355 We then used a state-of-the-art allometric equation established for tropical forests (37) to predict AGB from DBH
356 for natural forests in Rwanda:

357

358 $AGB_{\text{predicted}}$ in kg = $\exp[1.803 - 0.976E + 0.976 \ln(\rho) + 2.673 \ln(\text{DBH}) - 0.0299[\ln(\text{D})]^2]$ (E5)

359 Where E measures the environmental stress (37; a gridded layer is accessible via [https://chave.ups-](https://chave.ups-tlse.fr/pantropical_allometry.htm)
360 [tlse.fr/pantropical_allometry.htm](https://chave.ups-tlse.fr/pantropical_allometry.htm)), and ρ is the wood density which we set to 0.7 (58). No destructive AGB
361 measurements were found that showed a similar CD-DBH relationship as we measured during the field trip in
362 Rwanda's forest. We could thus not evaluate the performance for natural forests at tree level but had to rely on plot
363 level comparisons (next section).

364 **Evaluation and uncertainties of the allometry.** Biomass estimations without direct measurements of height or
365 DBH inevitably include a relatively high level of uncertainty at tree level (36,45,59). Uncertainty does not only
366 originate from the CD to DBH conversion but also the equation converting DBH to AGB. As shown in the previous
367 section, no strong systematic bias could be detected for the CD to DBH conversion, but the evaluation of the CD
368 based AGB prediction with an independent data set from destructively measured AGB revealed a bias of 25%.
369 However, this comparison (Extended Data | Fig. 3c) may not be representative for an entire country having a variety
370 of landscapes and tree species, so a systematic propagation is unlikely. We also did not have sufficient field data to
371 evaluate the conversions in natural forests. Here, we use data from 15 forest plots with 6,161 trees published by *ref.*
372 *41* and *ref. 42* and directly compared the summed biomass of the trees we predicted over their plots. The mean
373 measured biomass for the plots is 139 Mg C ha⁻¹ and we predict a mean biomass of 102 MgC ha⁻¹ (plot based RMSE
374 = 54%; bias = 11%; bias on summed plots = 26%). The overall underestimation by our prediction is not necessarily
375 a model bias but may be partly explained by the contribution of the understory trees, which cannot be captured by
376 aerial images. This number matches well with previously estimated contributions of understory to tropical intact
377 forests AGB (60). Interestingly, our AGC estimates are in the same range of magnitude as global forest biomass
378 products: (61,62,63,64,65) (Extended Data | Fig. 4), indicating that overstory tree level carbon stock assessments are
379 possible from optical very high resolution images, even in tropical forests. Interestingly, especially older global
380 products overestimated biomass for non-forest areas, which is likely because they rely more on optical data that
381 cannot distinguish between herbaceous and woody vegetation. The most recent product of *ref. 65* makes use of
382 spaceborne GEDI Lidar and provides values which are much closer to our estimations.

383 We further use NFI data from 2014 to evaluate if systematic differences between AGB predictions and field
384 assessments can be found for different land cover classes (Extended Data | Table 1). For the NFI data, a total of 373
385 plots with 2,415 trees were measured and species-specific allometric equations applied (66). Since the exact
386 locations of the plots were unknown, we extracted averaged values for areas close to the plots from our predictions
387 and calculated statistics on averages over all plots. Interestingly, our predictions for farmlands only show a bias of
388 5.9%: we estimate on average 2.46 Mg C ha⁻¹ and the inventories measure 2.37 Mg C ha⁻¹ on their 150 plots. For
389 savanna and shrublands, we estimate 4.16 Mg C ha⁻¹ while inventories measure 3.31 Mg C ha⁻¹ (bias = 18.9%). For
390 plantations, we estimate lower values (8.16 compared to 16.79 Mg C ha⁻¹; bias = 52.6%). To calculate the total
391 uncertainty on countrywide C stock estimates, we weighted the bias from the different classes according to their
392 relative area. We estimate a total bias of 16.9% at the national scale. (Extended Data | Table 1).

393 We found a very low bias for estimated C density in farmlands (5.9% bias) which make up most of the areas outside
394 natural forests in Rwanda (Extended Data | Table 1). The high bias for plantations can be explained by 3 factors:
395 large bare areas considered part of plantations (Extended Data | Table 1) by the manual delineation of plantation
396 areas; regular harvesting and continual thinning which keep many plantation trees young and small (39); and the
397 fact that our aerial images are from 2008, and plantation trees have grown rapidly until 2014 with a few new NFI
398 plots initiated after 2008. The bias in savannas and shrublands can be explained by the following factors: the
399 presence of multi-stemmed trees with large crowns such as *acacia spp*, *ficus spp*, among others; the fact that a crown-
400 based method overestimates C stocks of shrubs with a small height; and presence of shrub trees with both small
401 height and small (multiple) stems. If tree level based carbon stock assessments derived from crown diameter as
402 presented here should become standard to complement national inventories, a database with sufficient samples to

403 evaluate for systematic errors needs to be established for each biome, and inventory and satellite/aerial image based
404 methods need to be further harmonized.

405 To further quantify the error propagation of the CD to DBH conversion for our application, we established 4
406 equations each randomly using 50% of the dataset, and predicted the carbon stock for each tree in Rwanda with each
407 equation. We did this separately for natural forests and trees outside natural forests. We calculated the RMSE
408 between the aggregated carbon stocks for each hectare. We averaged the RMSE for each land cover class and show
409 that the uncertainty for all classes does not exceed 5% (Extended Data | Table 2).

410 **Evaluation and uncertainties of tree crown mapping.** We create an independent test dataset after the deep
411 learning model was finalized. This way, the test set was never seen during training and it was also not used to
412 optimize hyper-parameters. The test set consists of 153 random plots each 1 ha in size with a total of 6,591 manually
413 labeled trees (Extended Data | Fig. 6). The plot level comparison yielded very high correlations between the
414 predictions and the labels and is shown in Extended Data | Fig. 5. We also calculated a confusion matrix showing an
415 overall per pixel accuracy of 96.2%, a true positive rate of 79.6% and a false positive rate of 6.8% (Extended Data |
416 Table 3). Trees outside natural forests are easy to spot and count for the human eye, so we have confidence in the
417 plot based evaluation. However, it is often challenging in natural forests. Here we used again the field measurements
418 from 15 plots including 6,161 trees (41,42). We find that we underestimate the total tree count by 22.6%, which may,
419 at least partly, be explained by understory trees hidden by overstory trees and therefore not visible in our images.
420 Here, new field campaigns are needed to better understand and calibrate our results and possibly correct for
421 systematic bias.

422 **References**

- 423 1. Gamfeldt, L., Snäll, T., Bagchi, R. et al. Higher levels of multiple ecosystem services are found in forests with
424 more tree species. *Nat Commun* 4, 1340 (2013). <https://doi.org/10.1038/ncomms2328>
- 425 2. Morin, X., Fahse, L., Jactel, H. et al. Long-term response of forest productivity to climate change is mostly
426 driven by change in tree species composition. *Sci Rep* 8, 5627 (2018). <https://doi.org/10.1038/s41598-018-23763-y>
- 427
- 428 3. Tong, X., Brandt, M., Yue, Y. et al. Forest management in southern China generates short term extensive
429 carbon sequestration. *Nat Commun* 11, 129 (2020). <https://doi.org/10.1038/s41467-019-13798-8>
- 430 4. Tomppo, E., Gschwanter, Th., Lawrence, M., McRoberts, R.E. (Eds.) (2010). *National Forest Inventories*
431 *Pathways for Common Reporting*. Springer, 2010th edition
- 432 5. FAO. *National Forest Monitoring Systems: Monitoring and Measurement, Reporting and Verification (M &*
433 *MRV) in the context of REDD+ Activities*. Forest Assessment, Management and Conservation Division (2013),
434 Rome.
- 435 6. FAO. *Voluntary Guidelines on National Forest Monitoring*. Food and Agriculture Organization of the United
436 Nations (2017), Rome
- 437 7. UN. *The Global Forest Goals Report 2021*. United Nations Department of Economic and Social Affairs, United
438 Nations Forum on Forests Secretariat (2021). New York
- 439 8. UNFCCC. *Report of the Conference of the Parties on its twenty-first session, held in Paris from 30 November*
440 *to 13 December 2015*. 2016. Bonn
- 441 9. Stanturf, J.A., Kleine, M., Mansourian, S. et al. Implementing forest landscape restoration under the Bonn
442 Challenge: a systematic approach. *Annals of Forest Science* 76, 50 (2019). <https://doi.org/10.1007/s13595-019-0833-z>
- 443
- 444 10. Aleman, J., Blarquez, O., Gourlet-Fleury, S. et al. Tree cover in Central Africa: determinants and sensitivity
445 under contrasted scenarios of global change. *Sci Rep* 7, 41393 (2017). <https://doi.org/10.1038/srep41393>
- 446 11. Félix, G. F., Diedhiou, I., Le Graff, M., et al. Use and management of biodiversity by smallholder farmers in
447 semi-arid West Africa. *Glob. Food Sec* 18, 76-85 (2018). <https://doi.org/10.1016/j.gfs.2018.08.005>
- 448 12. Hansen, M. C., Potapo, P. V., Moore, R., et al. High-resolution global maps of 21st-century forest cover
449 change. *Science* 342, 850–853 (2013). <https://doi.org/10.1126/science.1244693>
- 450 13. Crowther, T., Glick, H., Covey, K. et al. Mapping tree density at a global scale. *Nature* 525, 201–205 (2015).
451 <https://doi.org/10.1038/nature14967>
- 452 14. Vancutsem, C., Achard, F., Pekel, J.F., Vieilledent, G., Carboni, S., Simonetti, D., Gallego, J., Aragão, L.E.O.C.,
453 Nasi, R. Long-term (1990–2019) monitoring of forest cover changes in the humid tropics. *Science Advances*
454 7(10), (2021), eabe1603. <https://doi.org/10.1126/sciadv.abe1603>
- 455 15. Brandt, M., Tucker, C.J., Kariryaa, A. et al. An unexpectedly large count of trees in the West African Sahara
456 and Sahel. *Nature* 587, 78–82 (2020). <https://doi.org/10.1038/s41586-020-2824-5>
- 457 16. Schnell, S., Kleinn, C. & Ståhl, G. Monitoring trees outside forests: a review. *Environ Monit Assess* 187, 600
458 (2015). <https://doi.org/10.1007/s10661-015-4817-7>
- 459 17. Mertz, O.; Grogan, K.; Pflugmacher, D.; Lestrelin, G.; Castella, J.-C.; Vongvisouk, T.; Hett, C.; Fensholt, R.;
460 Sun, Z.; Berry, N.; et al. Uncertainty in establishing forest reference levels and predicting future forest-based
461 carbon stocks for REDD+. *J. Land Use Sci.* 13, 1–15 (2018)
- 462 18. Rinaldi, F. & Johnson, R. Accounting for uncertainty in forest management models. *For. Ecol. Manag.* 468,
463 118186 (2020). <https://doi.org/10.1016/j.foreco.2020.118186>
- 464 19. Qin, Y., Xiao, X., Wigneron, JP. et al. Carbon loss from forest degradation exceeds that from deforestation in
465 the Brazilian Amazon. *Nat. Clim. Chang.* (2021). <https://doi.org/10.1038/s41558-021-01026-5>
- 466 20. Gross, D., Achad, F., Dubois, G., et al. Uncertainties in tree cover maps of Sub-Saharan Africa and their
467 implications for measuring progress towards CBD Aichi Targets. *Remote sens ecol con.* 4(2), 94-112 (2018).
468 <https://doi.org/10.1002/rse2.52>

- 469 21. Diakhite, M. AFR100 (the African Forest Landscape Restoration Initiative) is a country-led effort to bring 100
470 million hectares of land in Africa into restoration by 2030. African Union Development Agency-NEPAD.
471 Accessed on 11th June 2021. Available online: <https://afr100.org/>
- 472 22. FAO. From reference levels to results reporting: REDD+ under the United Nations Framework Convention on
473 Climate Change – 2020 update. (2020). Rome, FAO. <https://doi.org/10.4060/cb1635en>
- 474 23. Hansen, A.J., Burns, P., Ervin, J. et al. A policy-driven framework for conserving the best of Earth’s remaining
475 moist tropical forests. *Nat Ecol Evol* 4, 1377–1384 (2020). <https://doi.org/10.1038/s41559-020-1274-7>
- 476 24. Aleman, J.C., Jarzyna, M.A. & Staver, A.C. Forest extent and deforestation in tropical Africa since 1900. *Nat*
477 *Ecol Evol* 2, 26–33 (2018). <https://doi.org/10.1038/s41559-017-0406-1>
- 478 25. Benioff, R., Bazilian, M., Cox, S., Uriarte, C., Kecman, A., De Simone, G., Kitaoka, K., Ploutakhina, M. &
479 Radka, M. Low Emission Development Strategies: The Role of Networks and Knowledge Platforms. National
480 laboratory of the U.S. Department of Energy, Office of Energy Efficiency & Renewable Energy, NREL/TP-
481 6A00-55343, Denver West Parkway, Golden
- 482 26. Niang, I., Ruppel, O.C, Abdrabo, M.A. et al. Africa. In: *Climate Change 2014: Impacts, Adaptation, and*
483 *Vulnerability. Part B: Regional Aspects. Contribution of Working Group II to the Fifth Assessment Report of*
484 *the Intergovernmental Panel on Climate Change* [Barros, V.R., C.B. Field, D.J. Dokken, M.D. Mastrandrea, K.J.
485 Mach, T.E. Bilir, M. Chatterjee, K.L. Ebi, Y.O. Estrada, R.C. Genova, B. Girma, E.S. Kissel, A.N. Levy, S.
486 MacCracken, P.R. Mastrandrea, and L.L. White (eds.)]. Cambridge University Press (2014), Cambridge, United
487 Kingdom and New York, NY, USA, 1199-1265.
- 488 27. Dave, R., Saint-Laurent, C., Moraes, M., Simonit, S., Raes, L., Karangwa, C. Bonn Challenge Barometer of
489 Progress: Spotlight Report 2017, (2017). Gland, Switzerland: IUCN, 36ppSDGs
- 490 28. Republic of Rwanda. Rwanda Vision 2020 – Revised in 2012. The Republic of Rwanda, Ministry of Finance
491 and Economic Planning, Kigali (2012).
- 492 29. Nkurunziza, M. Rwanda reaches 30% forest cover target. *The New Times*, November 02, 2019. Accessed on
493 25th January 2021. Available online: <https://www.newtimes.co.rw/news/rwanda-reaches-30-forest-cover-target>
- 494 30. Stanturf, J.A., Kleine, M., Mansourian, S. et al. Implementing forest landscape restoration under the Bonn
495 Challenge: a systematic approach. *Annals of Forest Science* 76, 50 (2019). <https://doi.org/10.1007/s13595-019-0833-z>
- 496 31. REMA. State of the Environment and Outlook Report - Rwanda. Rwanda Environment Management Authority,
497 Kigali (2015)
- 498 32. Rwanyiziri, G. Relief and Hydrography. In D. Ben Yahmed and N. Houstin (Eds.), *Africa Atlases*. Rwanda,
499 Les Éditions du Jaguar, Paris, 7677 (2013)
- 500 33. Swedesurvey. Rwanda National Land Use and Development Master Plan - Report for Production of orthophoto
501 in Rwanda. Swedesurvey, Lantmäterigatan 2A, 802 64 Gävle (2010)
- 502 34. Nduwamungu, J., Nyandwi, E., Mazimpaka, J. D., Mugiraneza, T., Mukashema, A., Rwanyiziri, G., Nzabanita,
503 V. Rwanda forest cover mapping using high resolution aerial photographs. *The Global Geospatial Conference*
504 (2013), Addis Ababa, Ethiopia
- 505 35. Jucker, T., Caspersen, J., Chave, J. et al. Allometric equations for integrating remote sensing imagery into forest
506 monitoring programmes, *Global Change Biology*, 23(1), 177-190. <https://doi.org/10.1111/gcb.13388>
- 507 36. Kuyah, S., Dietz, J., Muthuri, C., et al. Allometric equations for estimating biomass in agricultural landscapes:
508 I. Aboveground biomass. *Agric. Ecosyst. Environ.* 158, 216– 224 (2012).
509 <http://dx.doi.org/10.1016/j.agee.2012.05.011>
- 510 37. Chave, J. et al. Improved allometric models to estimate the aboveground biomass of tropical trees. *Glob.*
511 *Change Biol.* 20, 3177–3190 (2014). <https://doi.org/10.1111/gcb.12629>
- 512 38. Mukuralinda, A., Kuyah, S., Ruzibiza, M. Allometric equations, wood density and partitioning of aboveground
513 biomass in the arboretum of Ruhunde, Rwanda. *Trees, Forests and People* 3, 100050 (2021).
514 <https://doi.org/10.1016/j.tfp.2020.100050>
- 515 39. Mugunga, C. P. The use of Eucalyptus in agroforestry systems of southern Rwanda: to integrate of segregate?
516 PhD thesis, Wageningen University, Wageningen, NL (2016)
- 517

- 518 40. Ndayambaje, J.D., Heijman, W.J.M. & Mohren, G.M.J. Farm woodlots in rural Rwanda: purposes and
519 determinants. *Agroforest Syst* 87, 797–814 (2013). <https://doi.org/10.1007/s10457-013-9597-x>
- 520 41. Nyirambangutse, B., Zibera, E., Uwizeye, F. K., Nsabimana, D., Bizuru, E., Pleijel, H., Uddling, J., and Wallin,
521 G. Carbon stocks and dynamics at different successional stages in an Afromontane tropical forest,
522 *Biogeosciences*, 14, 1285–1303(2017). <https://doi.org/10.5194/bg-14-1285-2017>.
- 523 42. Cuni-Sanchez, A., Sullivan, M.J.P., Platts, P.J. et al. High aboveground carbon stock of African tropical
524 montane forests. *Nature* 596, 536–542 (2021). <https://doi.org/10.1038/s41586-021-03728-4>
- 525 43. Castilla, G. and Hay, G. J. Uncertainties in land use data. *Hydrol. Earth Syst. Sci.*, 11, 1857–1868 (2007).
526 <https://doi.org/10.5194/hess-11-1857-2007>
- 527 44. Bastin, J-F., Finegold, Y., Garcia, C. The global tree restoration potential. *Science*, 365(6448), (2019).
528 <https://doi.org/10.1126/science.aax0848>
- 529 45. Skole, D.L., Samek, J.H., Dieng, M., & Mbow, C. The contribution of trees outside of forests to landscape
530 carbon and climate change mitigation in west africa. *Forests* 12, 1652 (2021).
531 <https://doi.org/10.3390/f12121652>
- 532 46. Romijn, E., De Sy, V., Herold, M., et al. Independent data for transparent monitoring of greenhouse gas
533 emissions from the land use sector – What do stakeholders think and need? *Environ Sci Policy* 85, 101-112
534 (2018). <https://doi.org/10.1016/j.envsci.2018.03.016>
- 535 47. Skole, D.L., Mbow, C., Mugabowindekwe, M. et al. Trees outside of forests as natural climate solutions. *Nat.*
536 *Clim. Chang.* 11, 1013–1016 (2021). <https://doi.org/10.1038/s41558-021-01230-3>
- 537 48. Sayre, R., Roca, E., Sedaghatkish, G. et al. *Nature in focus - rapid ecological assessment. The nature*
538 *conservancy, Island press, Washington (2000)*
- 539 49. CGIS. Rwanda forest cover mapping using high resolution aerial photographs. The “Programme d’Appui à la
540 Reforestation - Component funded by the Netherland (PAREF NL)”, Rwanda Natural Resources Authority
541 (2012)
- 542 50. Republic of Rwanda. Presidential Order establishing the National Land Use and Development Master Plan, N°
543 058/01 of 23/04/2021. Official Gazette n° 15 bis of 26/04/2021. Republic of Rwanda (2021).
- 544 51. Ronneberger, O., Fischer P. & Brox, T. U-net: convolutional networks for biomedical image segmentation. In
545 International Conference on Medical Image Computing and Computer-Assisted Intervention (eds. Navab, N. et
546 al.) 234–241, (Springer, 2015).
- 547 52. Koch, T., Perslev, M., Igel, C. & Brandt, S. Accurate segmentation of dental panoramic radiographs with U-nets.
548 In Proc. IEEE International Symposium on Biomedical Imaging (ISBI) (eds Davis, L. et al.) 15–19 (IEEE
549 Computer Society, 2019).
- 550 53. Brown, S., Gillespie, A. J. R. & Lugo, A. E. Biomass estimation methods for tropical forests and the application
551 to forest inventory data. *Forest Science* 35(4), 881-902 (1989)
- 552 54. Chave, J., Andalo, C., Brown, S. et al. Tree allometry and improved estimation of carbon stocks and balance in
553 tropical forests. *Oecologia* 145, 87–99 (2005). <https://doi.org/10.1007/s00442-005-0100-x>
- 554 55. IPCC. IPCC Guidelines for national greenhouse gas inventories, Prepared by the National Greenhouse Gas
555 Inventories Programme (2006), IGES, Japan
- 556 56. Martin, A.R., Doraisami, M. & Thomas, S.C. Global patterns in wood carbon concentration across the world’s
557 trees and forests. *Nature Geosci* 11, 915–920 (2018). <https://doi.org/10.1038/s41561-018-0246-x>
- 558 57. Baskerville, G. L. Use of logarithmic regression in the estimation of plant biomass. *Can. J. Forest Res.* 2, 49-53
559 (1972)
- 560 58. Bastin, J-F., Fayolle, A., Tareken, Y., et al. Wood specific gravity variations and biomass of central african tree
561 species: The simple choice of the outer wood. *PLOS ONE*, 10(11), e0142146 (2015).
562 <https://doi.org/10.1371/journal.pone.0142146>
- 563 59. Djomo, A. N., & Chimi, C. D. (2017). Tree allometric equations for estimation of above, below and total
564 biomass in a tropical moist forest: Case Study with Application to Remote Sensing. *Forest Ecology and*
565 *Management*, 381, 184-193. <https://doi.org/10.1016/j.foreco.2017.02.022>

- 566 60. Pan, Y., Birdsey, R. A., Fang, J. A large and persistent carbon sink in the world's forests. *Science* 333(6045),
567 988-993 (2011). <https://doi.org/DOI: 10.1126/science.1201609>
- 568 61. Santoro, M.; Cartus, O. (2021): ESA Biomass Climate Change Initiative (Biomass_cci): Global datasets of
569 forest above-ground biomass for the years 2010, 2017 and 2018, v2. Centre for Environmental Data Analysis,
570 17 March 2021. <http://dx.doi.org/10.5285/84403d09cef3485883158f4df2989b0c>
- 571 62. Baccini, A., Goetz, S., Walker, W. et al. Estimated carbon dioxide emissions from tropical deforestation
572 improved by carbon-density maps. *Nature Clim Change* 2, 182–185 (2012). <https://doi.org/10.1038/nclimate13>
- 573 63. Bouvet, A., Mermoz, S., Le Toan, T. et al (2018). An above-ground biomass map of African savannahs and
574 woodlands at 25m resolution derived from ALOS PALSAR. *Remote Sens. Environ.* 206, 156-173.
575 <https://doi.org/10.1016/j.rse.2017.12.030>
- 576 64. Hanan, N.P., L. Prihodko, C.W. Ross, G. Bucini, and A.T. Tredennick. 2020. Gridded Estimates of Woody
577 Cover and Biomass across Sub-Saharan Africa, 2000-2004. ORNL DAAC, Oak Ridge, Tennessee,
578 USA. <https://doi.org/10.3334/ORNLDAAAC/1777>
- 579 65. Xu, L., Saatchi, S., Yang, Y., et al. Changes in global terrestrial live biomass over the 21st century. *Science*
580 *Advances*, 7(27). <https://doi.org/10.1126/sciadv.abe9829>
- 581 66. RNRA. Execution of a National Forest Inventory - Technical report No. 8: Detailed Results Monitoring System
582 for Forests and Measuring Tree Growth. Rwanda Natural Resources Authority, Kigali (2016)
- 583 67. Hazel, D. & Bardon, R. Conversion factors for bioenergy - NC Woody biomass. Oak Ridge National
584 Laboratory, 2008. <https://content.ces.ncsu.edu/conversion-factors-for-bioenergy>
- 585
586
587

588 **Acknowledgments**

589 We thank the University of Rwanda for providing the very high resolution aerial imagery for the study. We also
590 acknowledge the support from the University of Copenhagen, University of Rwanda, Wildlife Conservation Society
591 of Rwanda, and IPRC Kitabi for the organization and supervision of the fieldwork. We also thank African Parks and
592 Nyungwe Management Company for issuing the permit to conduct field data collection in Nyungwe Afromontane
593 tropical rainforest.

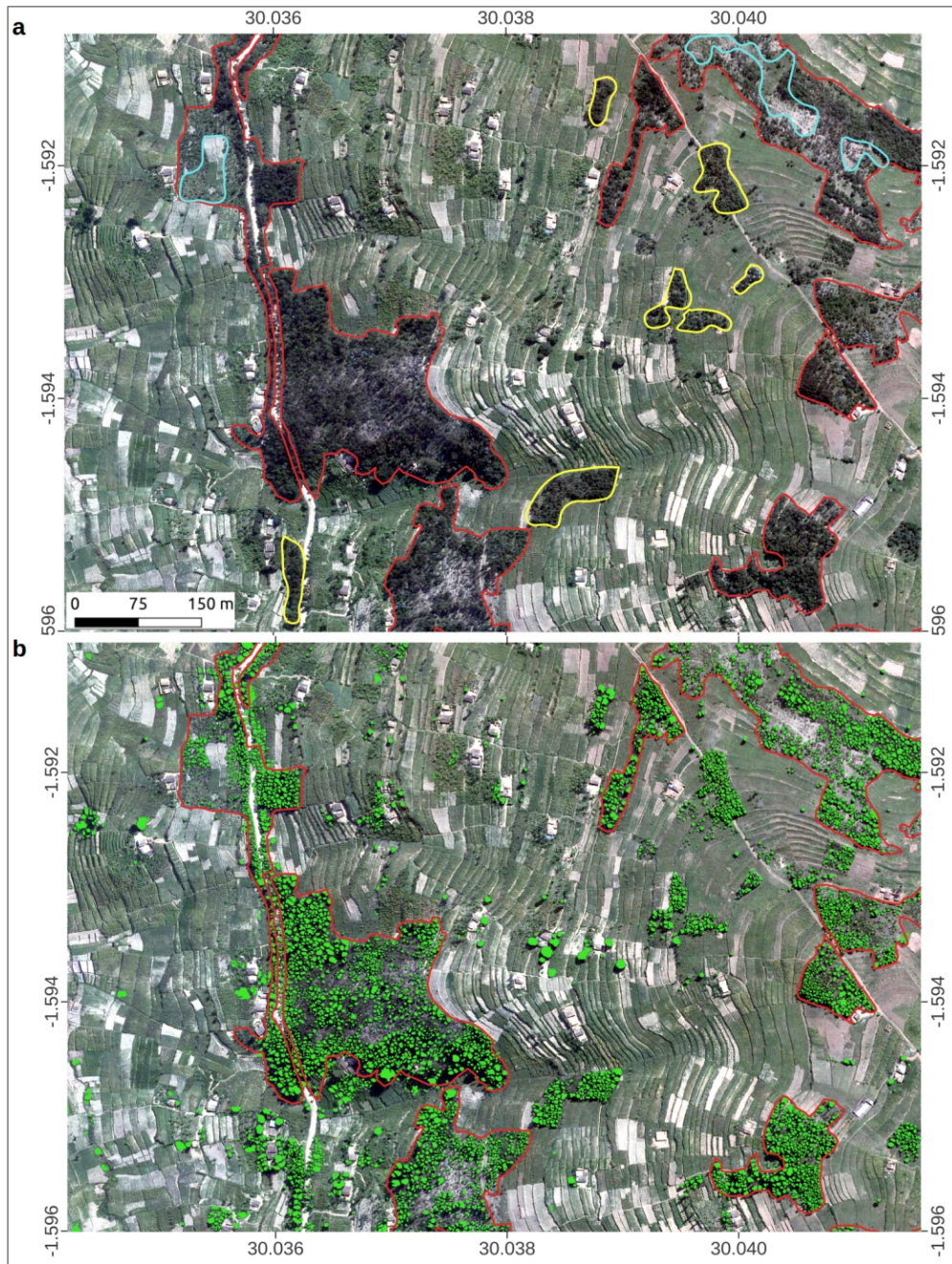
594 **Funding:** This work was funded by the European Research Council (ERC) under the European Union’s Horizon
595 2020 Research and Innovation Programme (grant agreement no. 947757 TOFDY) and DFF Sapere Aude (grant no.
596 9064–00049B). R.F., C.I., and A.K. acknowledge support by the Villum Foundation through the project Deep
597 Learning and Remote Sensing for Unlocking Global Ecosystem Resource Dynamics (DeReEco). C.I. acknowledges
598 support by the Pioneer Centre for AI, DNRF grant number P1.. J.C. acknowledges grants from “*Investissement*
599 *d’Avenir*” (CEBA, ref. ANR-10-LABX-25-01; TULIP, ref. ANR-10-LABX-0041), ESA CCI-Biomass and CNES”.
600 D.S. acknowledges support by NASA, grant no. 80NSSC21K0315 from the Land Cover and Land Use Change
601 Program. A.N. and V.U. acknowledge support by the European Union through the project Development of Smart
602 Innovation through Research in Agriculture (DeSiRa).

603 **Author contributions:** M.B., R.F. and M.M. designed the study. M.M. prepared and selected training and
604 validation dataset. A.K., S.L., F.R. wrote the code for the deep-learning framework, supported by F.G. and C.I.. A.K.
605 and C.I. wrote the code for post-processing framework to separate clumped trees. J.C. and D.S. prepared data from
606 existing tree measurements databases for carbon stocks related analyses. G.R. prepared aerial images. D.T. and V.U.
607 collected field data. A.N. and V.U. prepared NFI data. S.S. prepared the 2021 global estimates of above-ground
608 carbon stocks. M.M., M.B., J.C. and D.S. conducted the analyses. M.M., M.B., J.C., D.S., P.H., P.C., O.M., X.T.,
609 S.L., G.R., A.N., J-P. B. L., F.G., C.J.T., S.S. and R.F. conducted the interpretations. M.M. and M.B. wrote the first
610 manuscript draft with contributions by all authors. M.M. designed the figures.

611 **Competing interests:** The authors declare no competing interests.

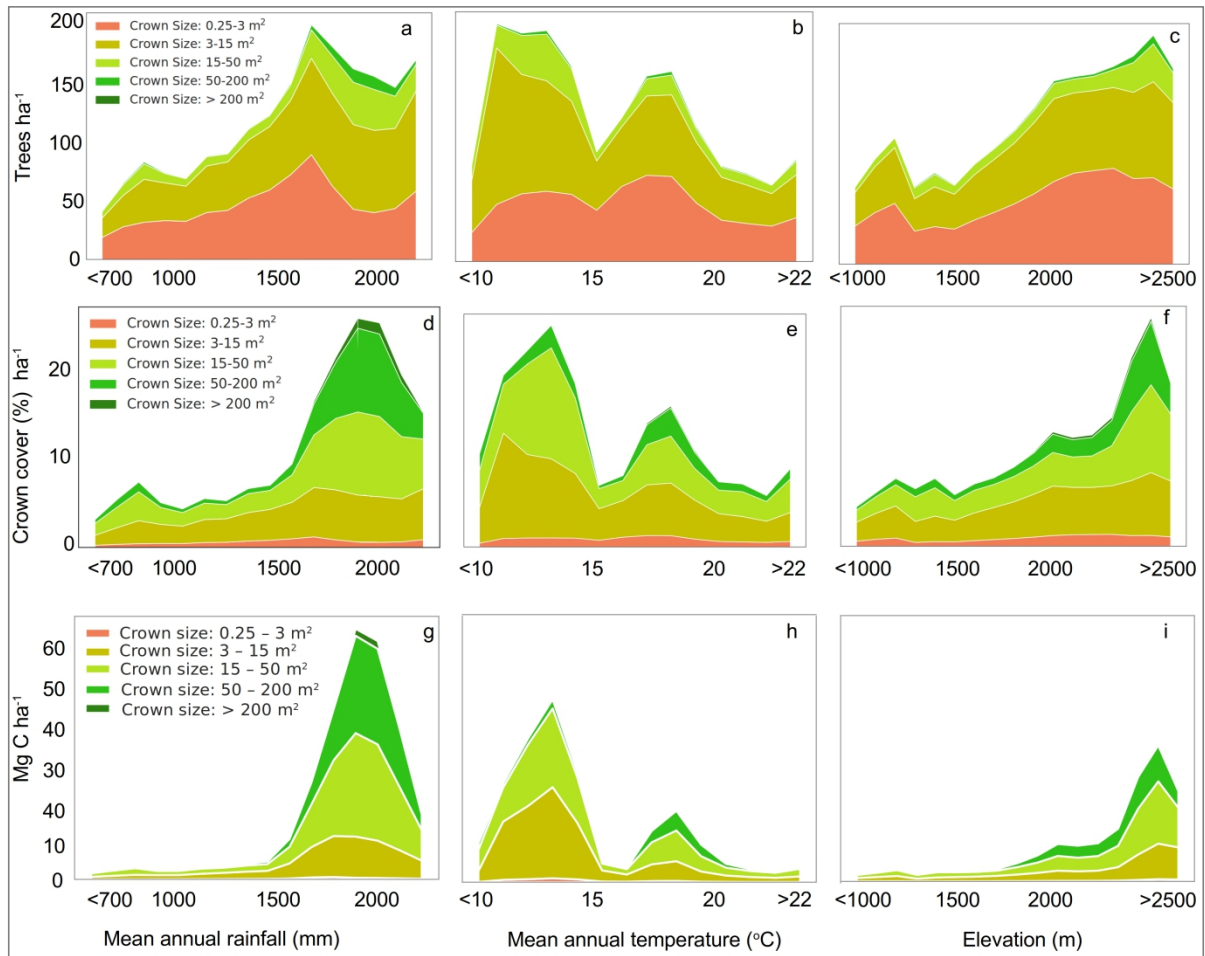
612 **Data availability:** Global tree cover maps are available at [http://earthenginepartners.appspot.com/science-2013-](http://earthenginepartners.appspot.com/science-2013-global-forest)
613 [global-forest](http://earthenginepartners.appspot.com/science-2013-global-forest). Climate data are freely accessible through online application to the Rwanda Meteorological Agency
614 via <http://mis.meteorwanda.gov.rw/>. Aerial images, and land use and land cover data are freely available for
615 research through formal application to the Rwanda Land Management and Use Authority: <https://www.rlma.rw>.
616 Individual tree maps produced in this article will be made public upon acceptance of the manuscript. The global
617 database with tree measurements including biomass is available from J.C.. Tree measurements from Kenya are
618 available from D.S.. Tree measurements from Rwanda are available from M.M.. The code for the tree detection
619 framework based on U-Net is publicly available at <https://doi.org/10.5281/zenodo.3978185>; support and more
620 information are available from A.K. (ak@di.ku.dk or ankit.ky@gmail.com) or F.R. (flr@ign.ku.dk). The code for
621 clumped trees separation framework is publicly available at https://github.com/ankitkarirya/separator_instances;
622 support and more information are available from A.K. or C.I. (igel@di.ku.dk). Any more relevant data can be
623 availed upon reasonable request addressed to the corresponding authors.

624



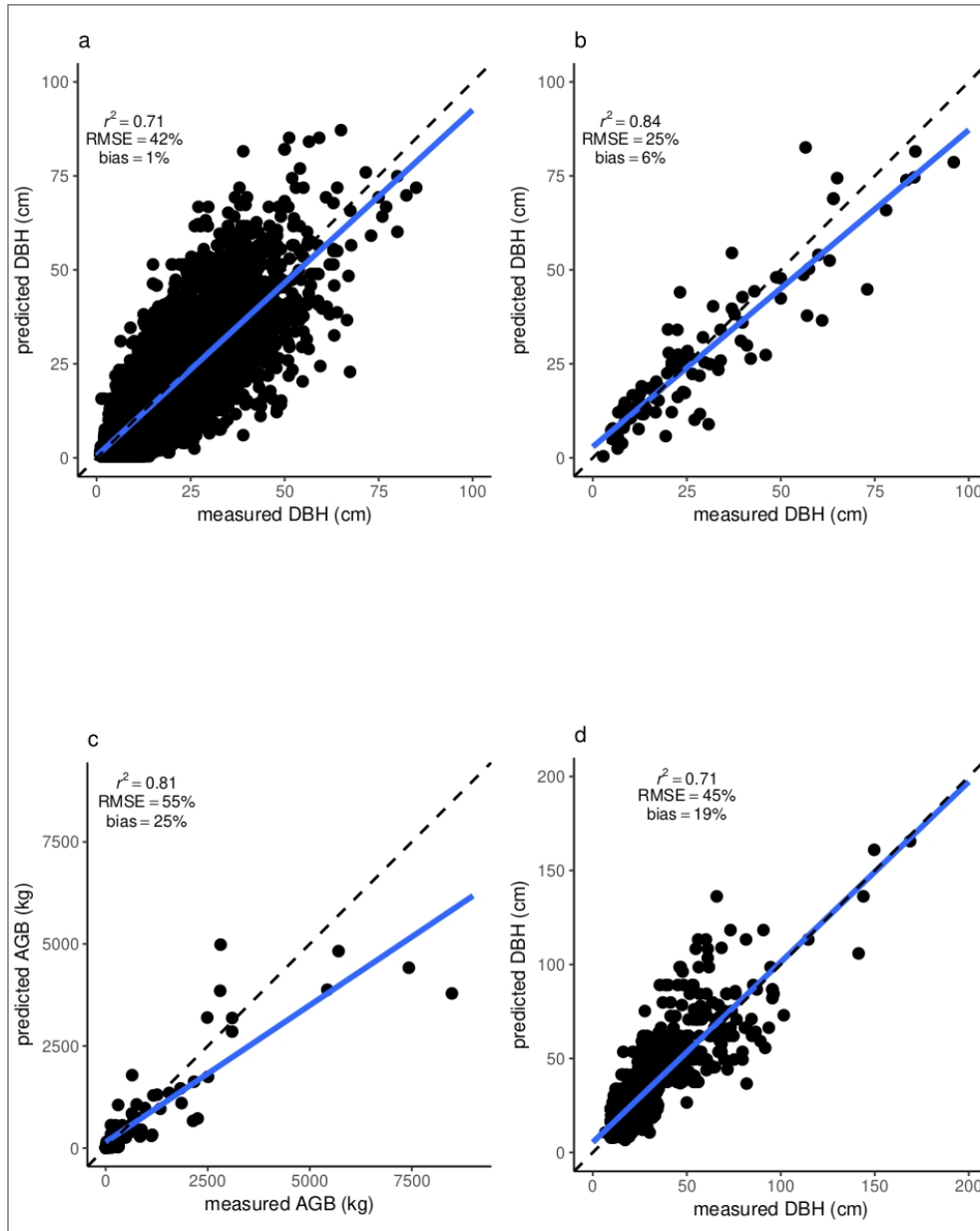
626
 627
 628
 629
 630
 631
 632

Extended Data | Fig. 1. An example showing previous manual forest delineations. The red lines are manually labeled forest boundary from the Rwanda national forest map of 2012 (49). **a**, Several patches which would qualify for the used forest definition were missed by the manual delineation (yellow lines). Also, some bare areas inside forest patches (cyan line) were considered as part of forests. **b**, Our results are shown in green, highlighting the improvements over the previous method.



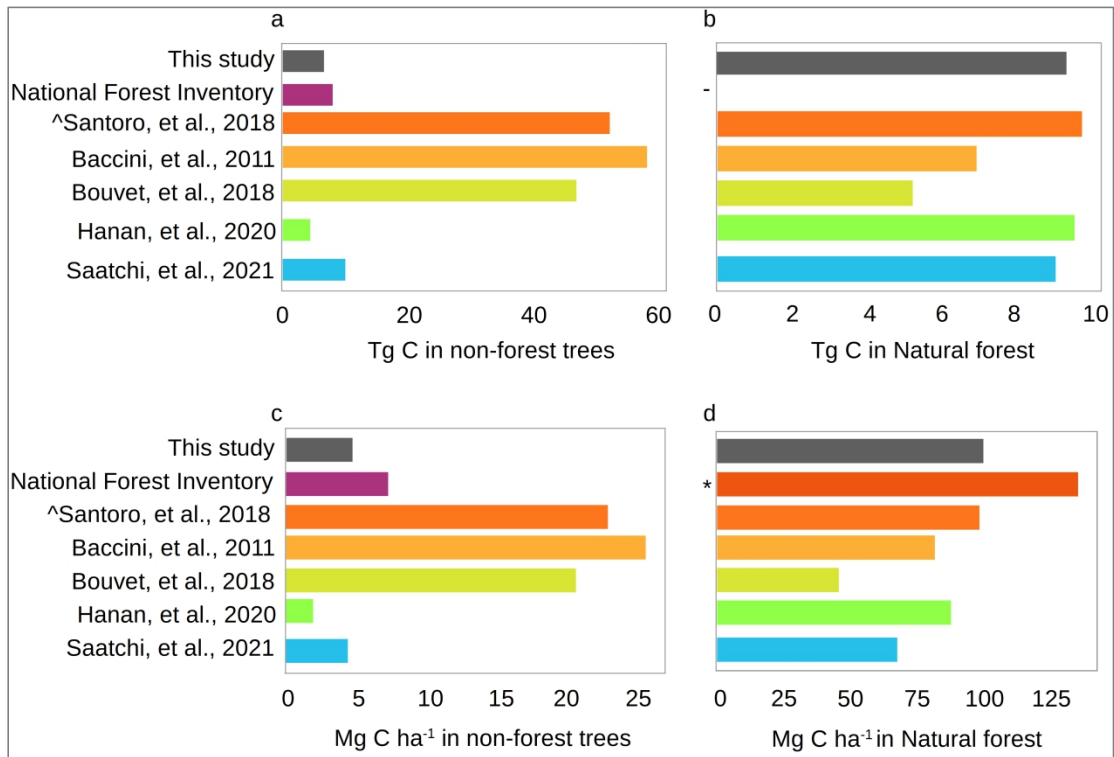
633
 634
 635
 636
 637
 638

Extended Data | Fig. 2. Tree characteristics related to different environmental factors. The variation of different crown sizes and their contribution to the total canopy cover along gradients of **a**, rainfall, **b**, temperature, and **c**, elevation. **d**, **e**, **f**, are the same as **a**, **b**, **c**, but for the mean crown cover. **g**, **h**, **i**, are the same as **a**, **b**, **c**, but for mean carbon stock ha^{-1} .



639
 640
 641
 642
 643
 644
 645
 646

Extended Data | Fig. 3. Tree crown allometry. **a**, DBH is predicted from CD using a total of 11,593 samples from a global database (35). The plot compares the predicted against the measured DBH. **b**, DBH is predicted for an independent dataset of 93 trees from Kenya using the equation derived from (a). **c**, We used an allometric equation from literature (36) to calculate AGB from the CD predicted DBH shown in (b). Predicted AGB is here compared with destructively measured AGB. **d**, While samples shown in a-c are all outside forests, (d) shows 793 field measured trees from Rwanda’s natural forest. As in (a), DBH was predicted from CD.



647

648

649

650

651

652

653

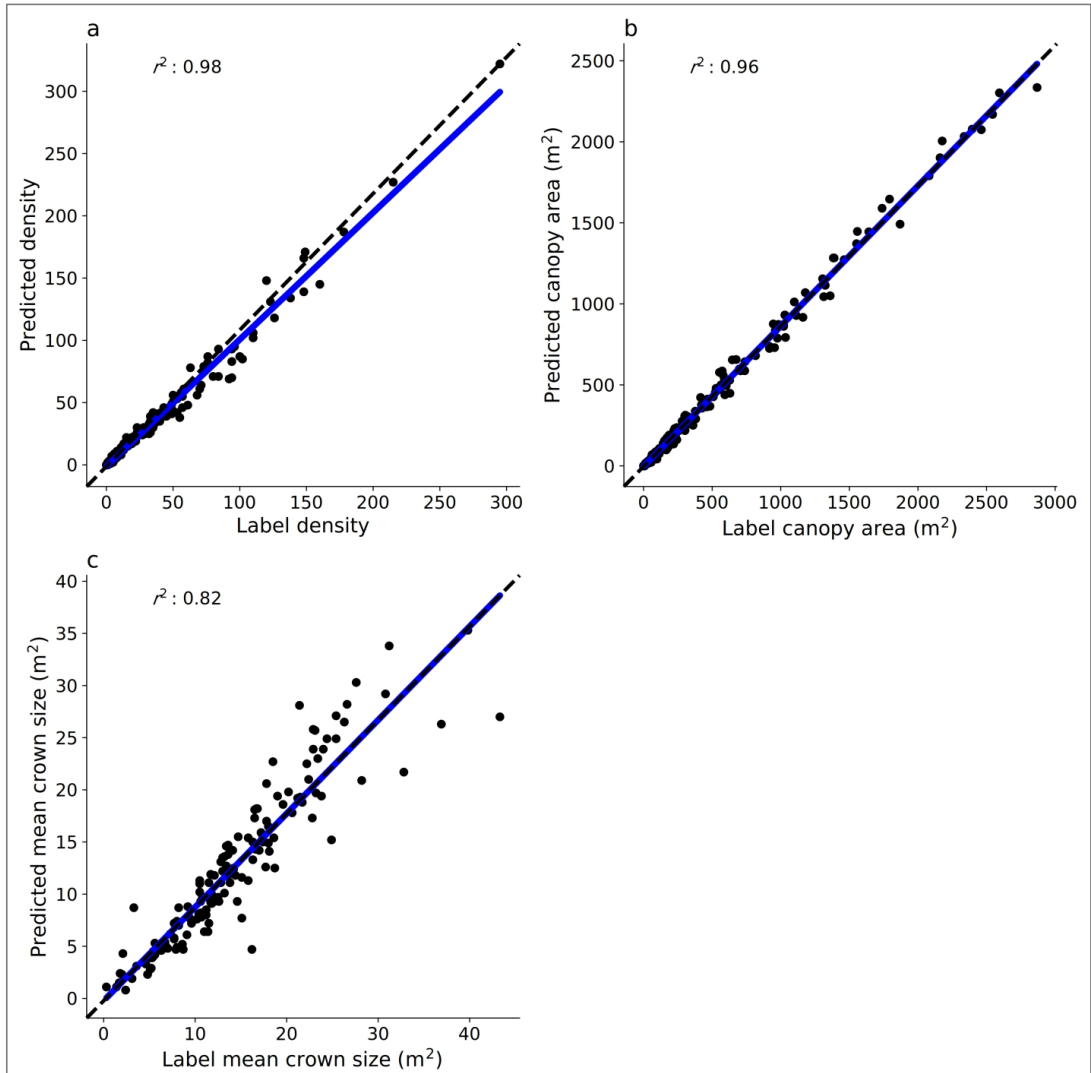
654

^ We selected the 2010 version

- Natural forest is not considered as part of the NFI

* Source: (20,21)

Extended Data | Fig. 4. Comparison of above-ground carbon estimations at country scale. a, Comparison of predicted total above-ground carbon stocks by this study, NFI and existing global products for non-forest areas. **b,** Same as (a) but for natural forests. **c,** Comparison of predicted above-ground carbon density by this study, NFI, and existing global products for non-forest areas. **d,** Same as (c) but for natural forests.



655

656 **Extended Data | Fig. 5. Tree crown model evaluation at plot level.** We manually labeled 6,591 trees in 153 plots
 657 and compared predictions and labeled trees at plot level. **a**, Tree density, **b**, canopy area, **c**, mean crown size. Each
 658 point represents one 1 ha plot.

659 **Extended Data | Table 1. Evaluation with field data.** We compared our tree level carbon stock estimates
 660 aggregated to 1 ha grids with field data from different sources. The exact location of the NFI plots was unknown, so
 661 we used averages of the areas close by. The statistics were then calculated for averages per class, except for natural
 662 forests where exact plot coordinates were available and comparisons could also be done per plot. We then weighted
 663 the bias according to the relative area at the national scale to derive a nation-wide uncertainty of 16.9%.

	Field data Mg C ha⁻¹	This study Mg C ha⁻¹	bias	Plots	Source	Relative area at national scale
Plantations	16.8	8.2	52.6%	106	NFI*	12%
Savanna and shrubland	3.3	4.2	18.9%	116	NFI*	33%
Farmland	2.4	2.5	5.9%	150	NFI*	48%
Natural forest	139	102	plots 11% sum 26%	15	Nyirambangutse, et al., 2017; Cuni-Sanchez, et al. (2021)	5%

664 * Note: The overall weighted national bias between NFI measurements and this study is 16.9% (NFI total C in TOF:
 665 8.35 Tg C; this study estimates 6.95 Tg C)

666 * The NFI original measurements are the above-ground biomass expressed in volume (m³). We have converted them
 667 in weight (metric tonnes) using the conversion rate: 1 m³ = 0.714 tonne (67) which assumes an overall average
 668 wood density of 0.714 g/cm³ per tree, and multiply by the AGB-to-AGC conversion factor: 0.47 (55,56) to get the
 669 C equivalent.
 670

671 **Extended Data | Table 2. Evaluation of the crown diameter to stem diameter conversion.** Four CD-DBH
672 equations were established, each using a random subset of 50% of the data. Tree biomass was predicted with each
673 equation and aggregated to the hectare level. We then calculated the RMSE and bias between the 4 predictions for
674 each 1 ha grid. Results shown here are aggregated over land cover classes.

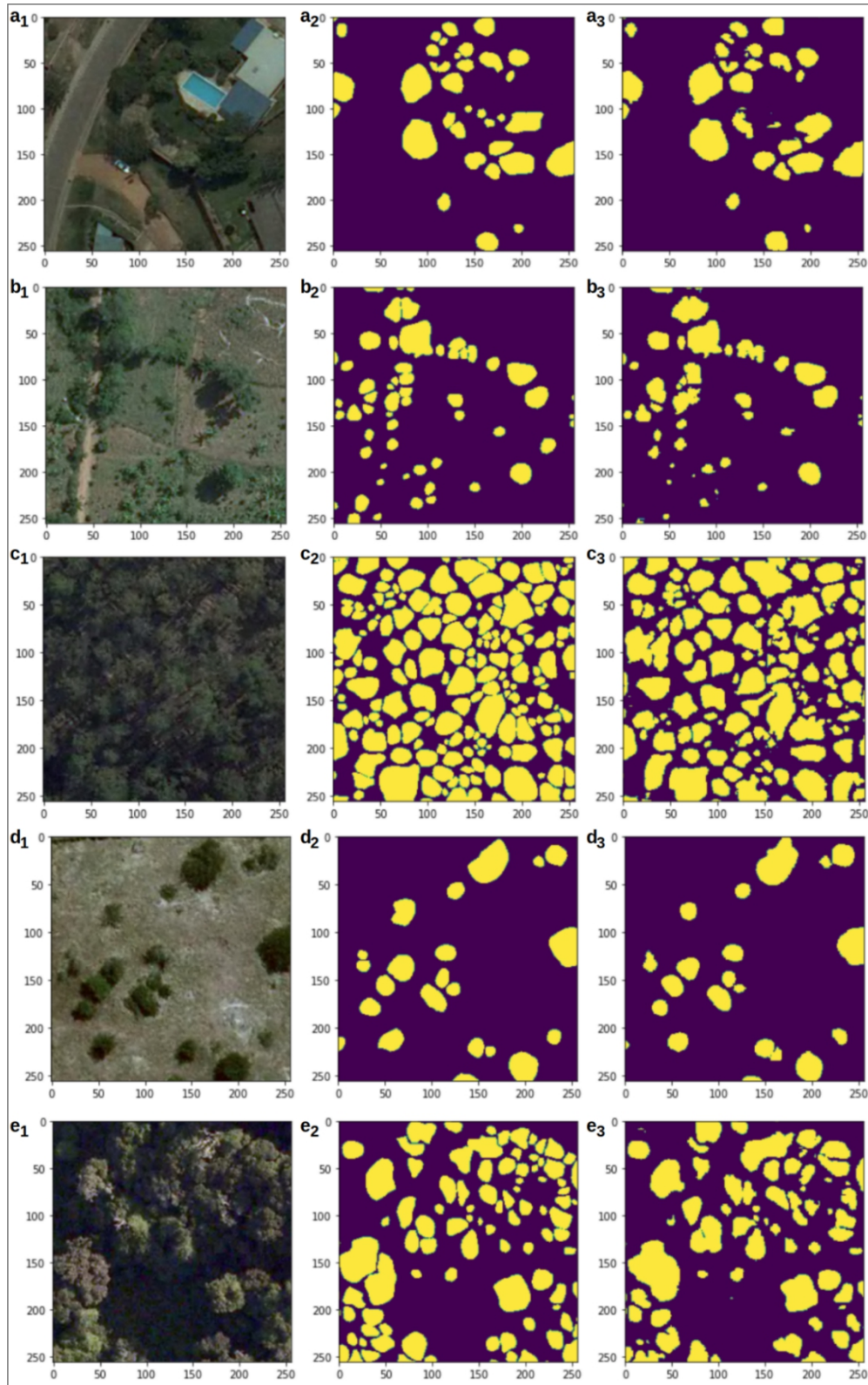
	RMSE (Mg C/ha)	Bias (%)
Farmland	0.08 (5%)	5.9
Savanna and shrubland	0.1 (5%)	5.1
Plantations (Eucalyptus)	0.2 (2%)	6.2
Plantations (non-Eucalyptus)	0.4 (2%)	3.9
Natural forest	1.7 (2%)	2.3

675

676 **Extended Data | Table 3. Tree crown model evaluation at pixel level.** Confusion matrix with 153 plots of 1 ha
677 size and 6,591 manually labeled trees. These data are independent and were not used to establish or validate the
678 model and the results.

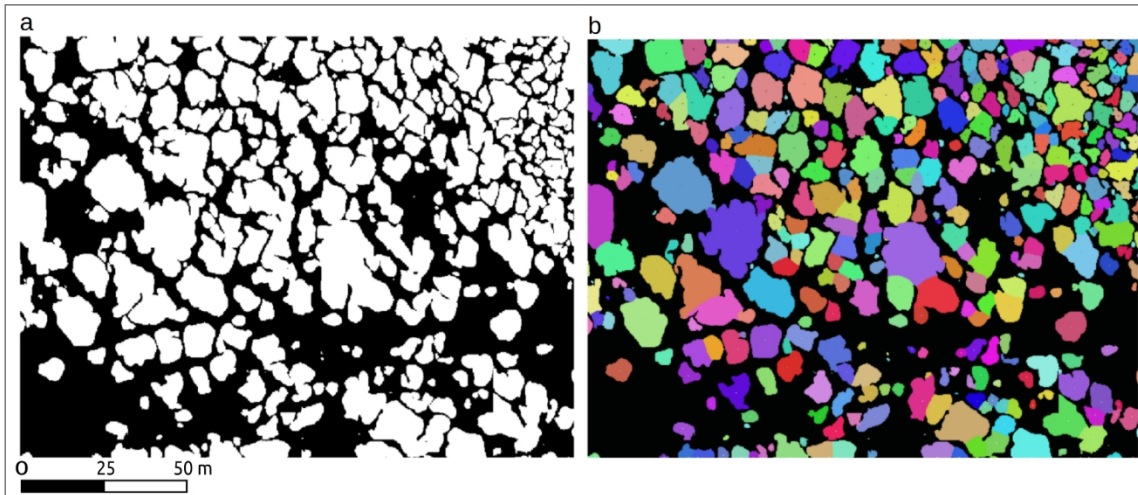
	Tree detected	No tree detected
Tree label exists	TP = 79.6%	FN = 20.4%
No tree label	FP = 6.8%	TN = 99.0%

679



680
681
682
683

Extended Data | Fig. 6. Illustration of sample independent plots for evaluating the deep learning model performance. **a**, Sample plot in a urban area, **b-e**, as in **(a)** but for **b**, farmlands, **c**, plantations, **d**, savanna and shrublands, **e**, natural forest. **1**, original image, **2**, manual tree crown labeling, **3**, deep learning model predictions.

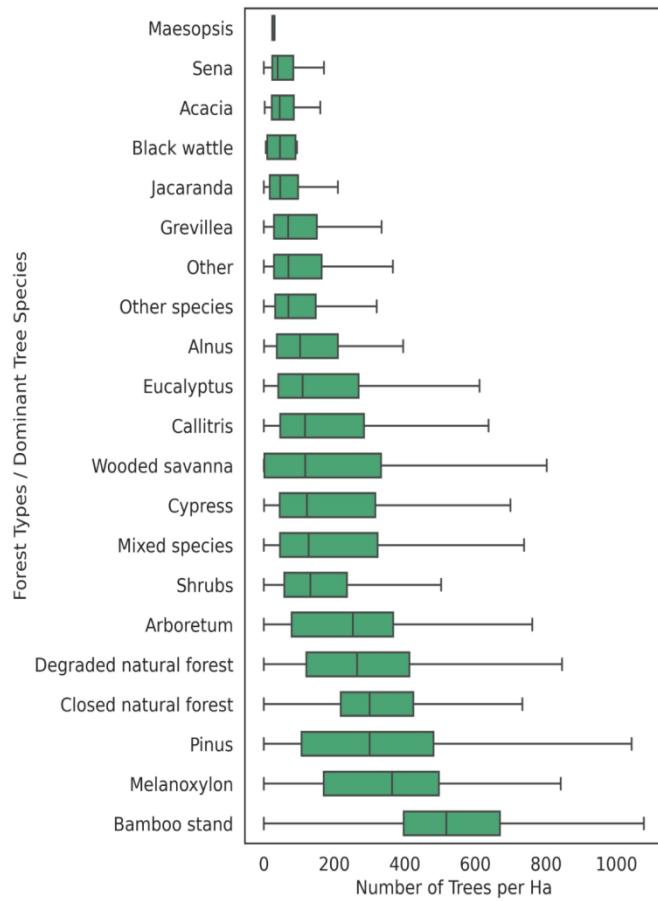


684
685 **Extended Data | Fig. 7. Examples from the post-processing algorithm separating clumped trees.** **a**, Example of
686 predicted tree crowns in the rainforest, with many trees being predicted as clumped objects. **b**, Results after the post-
687 processing algorithm separated the clumped crowns. The algorithm first finds the object centers, and then relabels
688 the image based on weighted distances to the identified centers. Thus, blobs containing multiple centers are divided
689 into various instances accordingly. The algorithm adds a large penalty for not-in-sight centers, and additionally
690 performs a majority filtering to remove the lone-pixels.

691
692



693
 694 **Extended Data | Fig. 8. Visual illustration of tree count and carbon stock per land cover type in Rwanda. a,**
 695 **Area size (1000 ha) covered by different land cover types, and b, tree count per land cover type (million trees), and c,**
 696 **carbon stocks per land cover type (Tg C). Although natural forests cover a small portion of land, they are home to a**
 697 **remarkable number of trees with the largest C stocks of the country**
 698



699
700
701
702
703

Extended Data | Fig. 9. Average tree density per tree species in Rwanda. Species data are from Rwanda national forest map of 2012 (49)